

Optic nerve astrocyte reactivity protects function in experimental glaucoma and other nerve injuries

Daniel Sun, Sara Moore, and Tatjana C. Jakobs

Department of Ophthalmology, Massachusetts Eye and Ear Infirmary/Schepens Eye Research Institute, Harvard Medical School, Boston, MA 02114

Reactive remodeling of optic nerve head astrocytes is consistently observed in glaucoma and other optic nerve injuries. However, it is unknown whether this reactivity is beneficial or harmful for visual function. In this study, we used the Cre recombinase (Cre)–*loxP* system under regulation of the mouse glial fibrillary acidic protein promoter to knock out the transcription factor signal transducer and activator of transcription 3 (STAT3) from astrocytes and test the effect this has on reactive remodeling, ganglion cell survival, and visual function after experimental glaucoma and nerve crush. After injury, *STAT3* knockout mice displayed attenuated astrocyte hypertrophy and reactive remodeling; astrocytes largely maintained their honeycomb organization and glial tubes. These changes were associated with increased loss of ganglion cells and visual function over a 30-day period. Thus, reactive astrocytes play a protective role, preserving visual function. *STAT3* signaling is an important mediator of various aspects of the reactive phenotype within optic nerve astrocytes.

INTRODUCTION

Glaucoma is the second leading cause of blindness worldwide, affecting an estimated 70 million people (Quigley, 2011; Pascolini and Mariotti, 2012). It causes a progressive and irreversible loss of retinal ganglion cells, leading to visual loss and blindness. The exact molecular mechanisms involved in this damage are not yet fully elucidated (Nickells et al., 2012). An elevated intraocular pressure (IOP) is the most important risk factor in glaucoma, and current medications focus on lowering the IOP. However, this is not always effective, with many patients continuing to progress in the disease even after IOP lowering. As yet, there are no clinically approved neuroprotective treatments that directly target the pathogenic mechanisms in the retina or optic nerve; IOP-lowering treatments address a risk factor. An important step toward finding alternative treatments is to better understand the pathogenic mechanisms underlying glaucoma. This involves going beyond studying the ganglion cells themselves to understand the potential role that nonneuronal cell types have in supporting the ganglion cells, including glial cells such as astrocytes.

The optic nerve head is an important site for early glaucomatous damage; there are profound alterations in tissue composition and architecture, disruptions in axonal transport, and critical axonal insult (Minckler et al., 1977; Johnson et al., 1996; Pease et al., 2000; Burgoyne et al., 2004; Jakobs et al., 2005; Balaratnasingam et al., 2007; Howell et al., 2007; Buckingham et al., 2008; Soto et al., 2008; Chidlow et al., 2011). Furthermore, the characteristic pattern of ganglion cell loss in glaucomatous retinas is best explained by a requirement for

damage to axon bundles in the optic nerve head (Schlamp et al., 2006; Howell et al., 2007). Ganglion cell axons exit the eye through a scleral opening that contains, depending on the species, a lamina cribrosa or a glial lamina. In humans, the lamina cribrosa is formed by a series of collagenous sieve-like plates through which bundles of ganglion cell axons pass. The surface of the plates and the pores are covered by a dense network of astrocytes (Hernandez et al., 2008). In the glial lamina of mice and rats, there is very little collagen, and instead, the axon bundles pass through pores that are formed by a dense network of astrocytes; hence, this arrangement has been termed the glial lamina (May and Lütjen-Drecoll, 2002; Howell et al., 2007; Sun et al., 2009). In either case, the lamina region is densely populated with astrocytes.

In a normal state, astrocytes support the axons they ensheath, but in response to injury/disease, they remodel and become reactive, inducing changes in morphology, gene expression, and function that have the potential for both beneficial and detrimental effects (Sofroniew and Vinters, 2010). Some of these reactive changes may include hypertrophy, proliferation, migration, release of extracellular matrix, up-regulation of complement and intermediate filaments (e.g., glial fibrillary acidic protein [GFAP], vimentin, and nestin), and scar formation (Hernandez, 2000; Sun et al., 2010; Sun and Jakobs, 2012; Lye-Barthel et al., 2013). Reactive remodeling is consistently observed in human and animal models of glaucoma (Morrison et al., 1990; Quigley et al., 1991; Hernandez and Ye, 1993; Johnson et al., 2007; Hernandez et al., 2008; Burgoyne, 2011). A long-standing question in glaucoma research is whether reactive astro-

Correspondence to Daniel Sun: daniel_sun@meei.harvard.edu

Abbreviations used: cIOP, cumulative IOP; CKO, conditional KO; ERG, electroretinogram; GFAP, glial fibrillary acidic protein; IOP, intraocular pressure; OHT, ocular hypertension; PPD, paraphenylenediamine; pSTR, positive STR; RT, room temperature; STR, scotopic threshold response.

© 2017 Sun et al. This article is distributed under the terms of an Attribution–Noncommercial–Share Alike–No Mirror Sites license for the first six months after the publication date (see <http://www.rupress.org/terms/>). After six months it is available under a Creative Commons License (Attribution–Noncommercial–Share Alike 4.0 International license, as described at <https://creativecommons.org/licenses/by-nc-sa/4.0/>).



cytes in the lamina region are harmful or beneficial for visual outcome. Although most agree that astrocytes do play an important role, current data fall short of demonstrating what this role is, and the function and mechanism of reactivity have not been studied.

STAT3 is a critical regulator of astrocyte reactivity and glial scar formation in both the brain and spinal cord (Herrmann et al., 2008; Wanner et al., 2013; Zhang et al., 2013; O'Callaghan et al., 2014; Ben Haim et al., 2015; Wong et al., 2015). STAT3 is a member of the Jak-STAT signaling family and is activated by phosphorylation through several cytokines and growth factors implicated in the injury response, including IL-6, ciliary neurotrophic factor, leukemia inhibitory factor, epidermal growth factor, and transforming growth factor α (Balasingam et al., 1994; Winter et al., 1995; Klein et al., 1997; Rabchevsky et al., 1998; Levison et al., 2000; Aaronson and Horvath, 2002). Astrocytes in the optic nerve, brain, and spinal cord all express STAT3, and its activation increases markedly after injuries and diseases such as trauma, ischemia, inflammation, neurodegenerative diseases, and in a rat model of transient elevation in IOP (Cattaneo et al., 1999; Acarin et al., 2000; Justicia et al., 2000; Sriram et al., 2004; Yamauchi et al., 2006; Zhang et al., 2013; Ben-Haim et al., 2015). In the injured brain and spinal cord, conditional KO (CKO) of *STAT3* or its extracellular receptor gp130 from astrocytes attenuated the injury-induced reactive phenotype, minimizing cellular hypertrophy, GFAP up-regulation, and scar formation (Okada et al., 2006; Drögemüller et al., 2008; Herrmann et al., 2008; Haroon et al., 2011; Wanner et al., 2013).

Using the same transgenic strategy as in the brain and spinal cord, we aimed to determine whether attenuating astrocyte reactivity in the optic nerve head after experimental glaucoma improves or worsens ganglion cell survival and visual function. We used the Cre recombinase (Cre)-*loxP* system under regulation of the mouse *GFAP* promoter to conditionally knock out *STAT3* from astrocytes and test the effect this has on astrocyte reactivity, ganglion cell survival, and visual function after transient ocular hypertension (OHT), chronic OHT, and an optic nerve crush. The transient OHT model represents a subtle mild injury that mimics the early stages of glaucoma (Crowston et al., 2015). Chronic OHT was induced via a microbead injection and gives a sustained chronic elevation in IOP (Sappington et al., 2010; Chen et al., 2011; Gao and Jakobs, 2016). A severe nerve crush model was used to determine how robust the effects of a *STAT3* KO were.

We report that knocking out *STAT3* attenuated astrocyte reactivity after experimental glaucoma and nerve crush, and this was associated with an increased loss of ganglion cells and visual function. Therefore, astrocyte reactivity plays a protective role in these injuries, supporting ganglion cell survival. Our results provide mechanistic and functional insight into the role of reactive astrocytes in the optic nerve head.

RESULTS

The normal appearance and visual function of GFAP-STAT3-CKO mice

The glial lamina of GFAP-STAT3-CKO mice was indistinguishable from GFAP-STAT3-Cre⁻ (control strain) and C57BL/6 mice (Fig. 1, A-I'). In all three mouse strains, a transverse cross section of this region showed astrocyte processes labeled with GFAP forming glial tubes through which ganglion cell axons pass (Fig. 1, A-B, D-E, and G-H; red dashed ellipses show such glial tubes; Howell et al., 2007; Sun et al., 2009). Numerous thick primary processes bundle to form the walls of the glial tubes (Fig. 1 A', arrowheads), and thinner processes run into the center of the tubes (Fig. 1 A', arrows). This arrangement gives the glial lamina an overall honeycomb appearance, with the center of the glial tubes having more process-free area. Ultrastructural examination of the GFAP-STAT3-CKO glial lamina showed that axonal morphology and organization was similar to the other two strains; all have similar-sized axons and a normal complement of microtubules and neurofilaments (Fig. 1, C, C', E, F', I, and I'). Several other histological and functional features of the three mouse strains were compared, and they were all indistinguishable from each other. These included: the IOPs, the number of ganglion cells, the spatial frequency threshold, and the electroretinogram (ERG) response (Fig. S1).

As a preliminary measure, we sought to determine whether the IOP of *STAT3* KO-transgenic mice would behave in a similar manner to C57BL/6 mice after microbead injection. After successful injections (Fig. S2 A), the pattern and duration of IOP elevation were the same in all three mouse strains and consistent with published results (Fig. S2 B; Chen et al., 2011; Della Santina et al., 2013; Gao and Jakobs, 2016). Furthermore, there was no statistical difference in the Δ cumulative IOP (Δ cIOP) or peak IOP reached, indicating that all animals received comparable pressure insult (see the Chronic OHT section of Materials and methods and Fig. S2 D).

Injury induces an early up-regulation of pSTAT3 in astrocytes of the glial lamina but not in retinal astrocytes

Untreated mice displayed immunohistochemically undetectable levels of pSTAT3 (Fig. 2, A-C). Injury induced an early up-regulation of pSTAT3 in many astrocytes, identified by their characteristic transversely elongated nuclei (Fig. 2, D-AA, arrows), which were enwrapped by GFAP-labeled processes (Fig. 2 E', arrows). Moreover, pSTAT3 labeling was completely abolished in the GFAP-STAT3-CKO mice, further indicating that the up-regulation was exclusively in astrocytes (not depicted). Transient OHT induced an up-regulation of pSTAT3 at days 1 and 3, followed by a return to normal by day 7 (Fig. 2, D-K). Chronic OHT similarly induced an up-regulation at day 1, but this was maintained through to at least day 7 (Fig. 2, L-S). Optic nerve crush induced a different time course of STAT3 activation. Phosphorylated STAT3 was up-regulated as early as 4 h after crush and lasted only until day 3 (Fig. 2, T-AA).

Next, we sought to determine whether there was any change in STAT3 immunoreactivity within the glial lam-

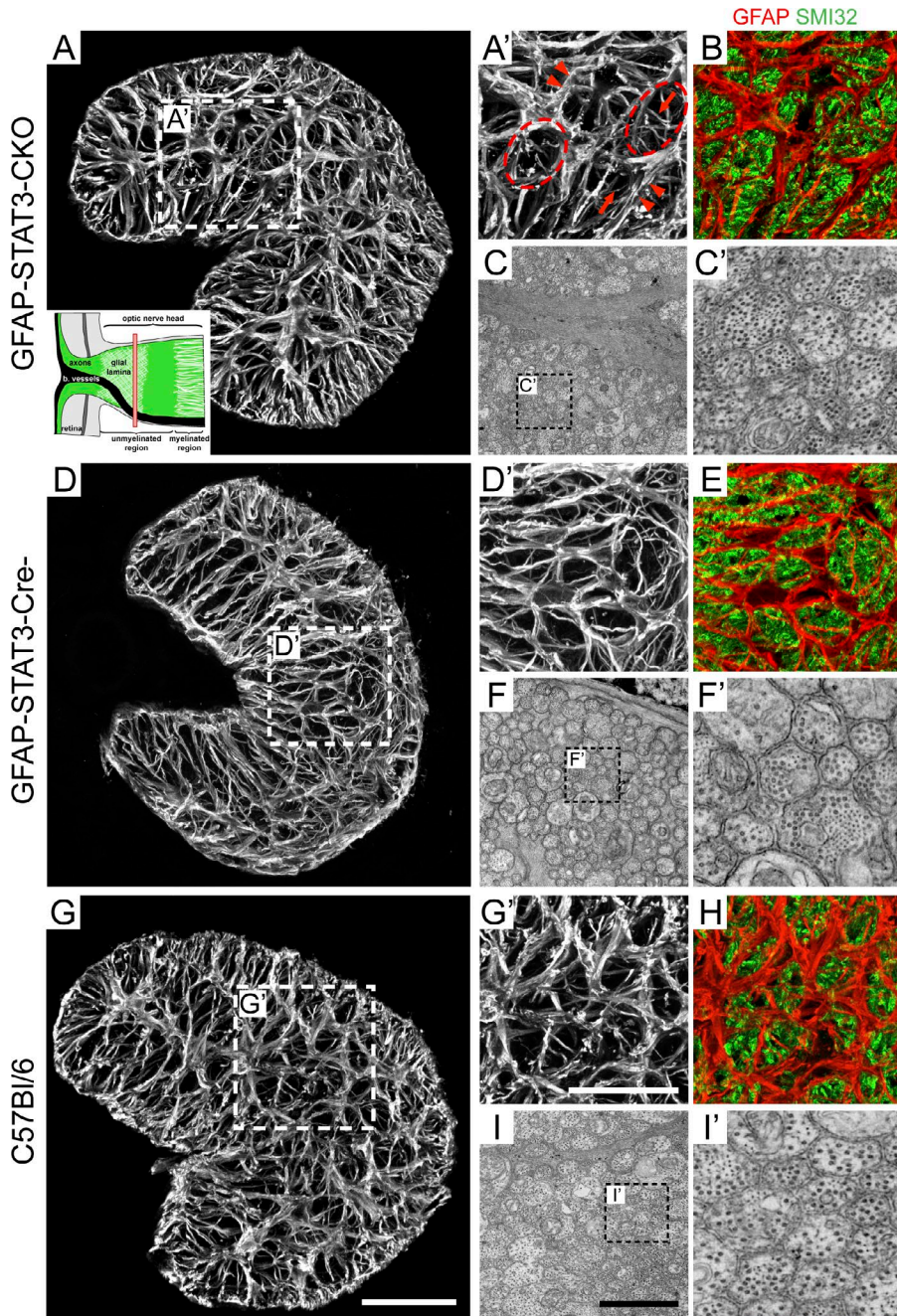


Figure 1. **Untreated GFAP-STAT3-CKO mice have a glial lamina that appeared similar to its control strain and C57BL/6 mice.** (A–B, D–E, and G–H) Transverse cross sections of optic nerves from the different mouse strains labeled for GFAP alone (A, A', D, D', G, and G') or colocalized with SMI32 (B, E, and H). (A, inset) The red bar in the schematic of the optic nerve head indicates where the transverse sections have been made. Arrows indicate the thin processes of astrocytes, arrowheads indicate the thick main processes, and the dashed ellipses indicate glial tubes. (C, C', F, F', I, and I') Ultrastructural examination of the optic nerve showing the axon-astrocyte organization and their morphology. Each panel represents a typical finding from a sample of three to five mice. Bars: (A, D, and G) 50 μm ; (A', B, D', E, G', and H) 20 μm ; (C, F, and I) 2 μm .

ina and whether STAT3 was activated in retinal astrocytes and Müller cells. We focused our analysis on mice subjected to chronic OHT and at days 1 and 3 after injury, a time when there was discernible up-regulation of pSTAT3 within the glial lamina. As expected from a previous study (Zhang et al., 2013), chronic OHT did not alter STAT3 immunoreactivity in any of the mouse strains, including the GFAP-STAT3-CKO strain at 1 or 3 d after injury (data depicted only for day 3; Fig. 3, A–D). Injury induced low-level up-regulation of pSTAT3 in many retinal cell types (chronic OHT: Fig. 3, F–H and J–L; optic nerve crush:

Fig. 3, M–O). However, we were surprised to find that, after chronic OHT, there were undetectable levels in astrocytes of GFAP-STAT3-Cre⁻ and C57BL/6 retinas (data depicted only for day 3; Fig. 3, F and G), despite the discernible up-regulation within astrocytes of the glial lamina at these time points. Furthermore, these retinal astrocytes were not significantly reactive (Fig. 3, E–H). As expected, there was no pSTAT3 labeling in astrocytes of GFAP-STAT3-CKO retinas (Fig. 3 H). In contrast to the astrocytes, Müller cells in all mouse strains showed an up-regulation of pSTAT3 (Fig. 3, J–L) and were reactive, as some of their processes

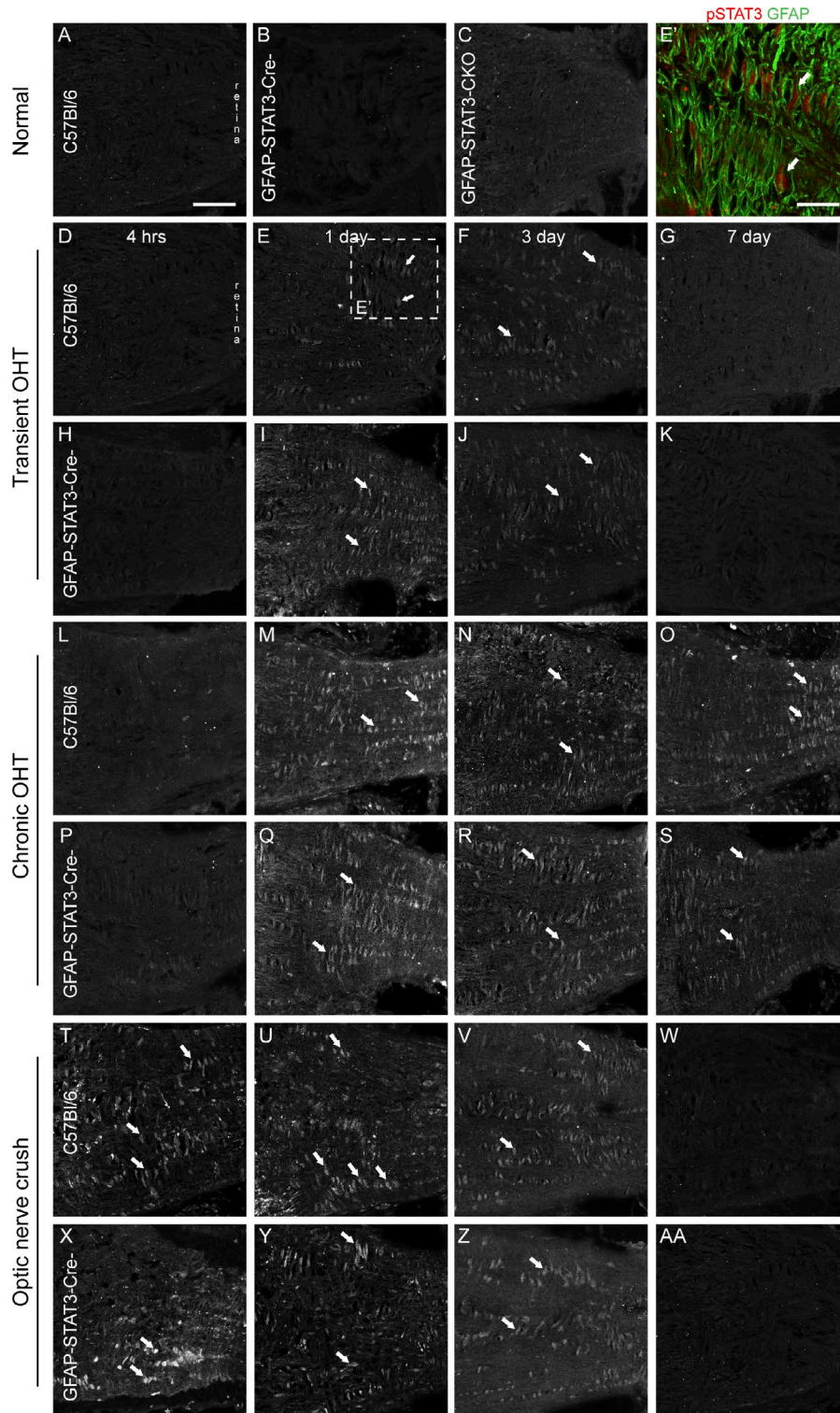


Figure 2. Injury induces an early up-regulation of pSTAT3 in astrocytes of the glial lamina. (A-AA) Longitudinal sections of the optic nerve head from the different mouse strains and injuries stained for pSTAT3 (arrows). (E') An enlargement from E showing colocalization of pSTAT3 with GFAP-labeled astrocytes. At no time after injury was there pSTAT3 labeling in GFAP-STAT3-CKO mice (not depicted). Each panel represents a typical finding from a sample of three to five mice. Bars: (A-AA, except E') 50 μ m; (E') 10 μ m.

became immunoreactive for GFAP (Fig. 3, F-H). Interestingly, severe injuries such as an optic nerve crush induced distinct pSTAT3 up-regulation within astrocytes in both the GFAP-STAT3-Cre⁻ and C57BL/6 mice but not in the GFAP-STAT3-CKO mice (Fig. 3, M-O).

Attenuated astrocyte reactivity and remodeling in GFAP-STAT3-CKO glial lamina

Next, we determined the effect that knocking out *STAT3* has on astrocyte reactivity within the glial lamina by examining GFAP immunoreactivity. We assessed the reorganization of

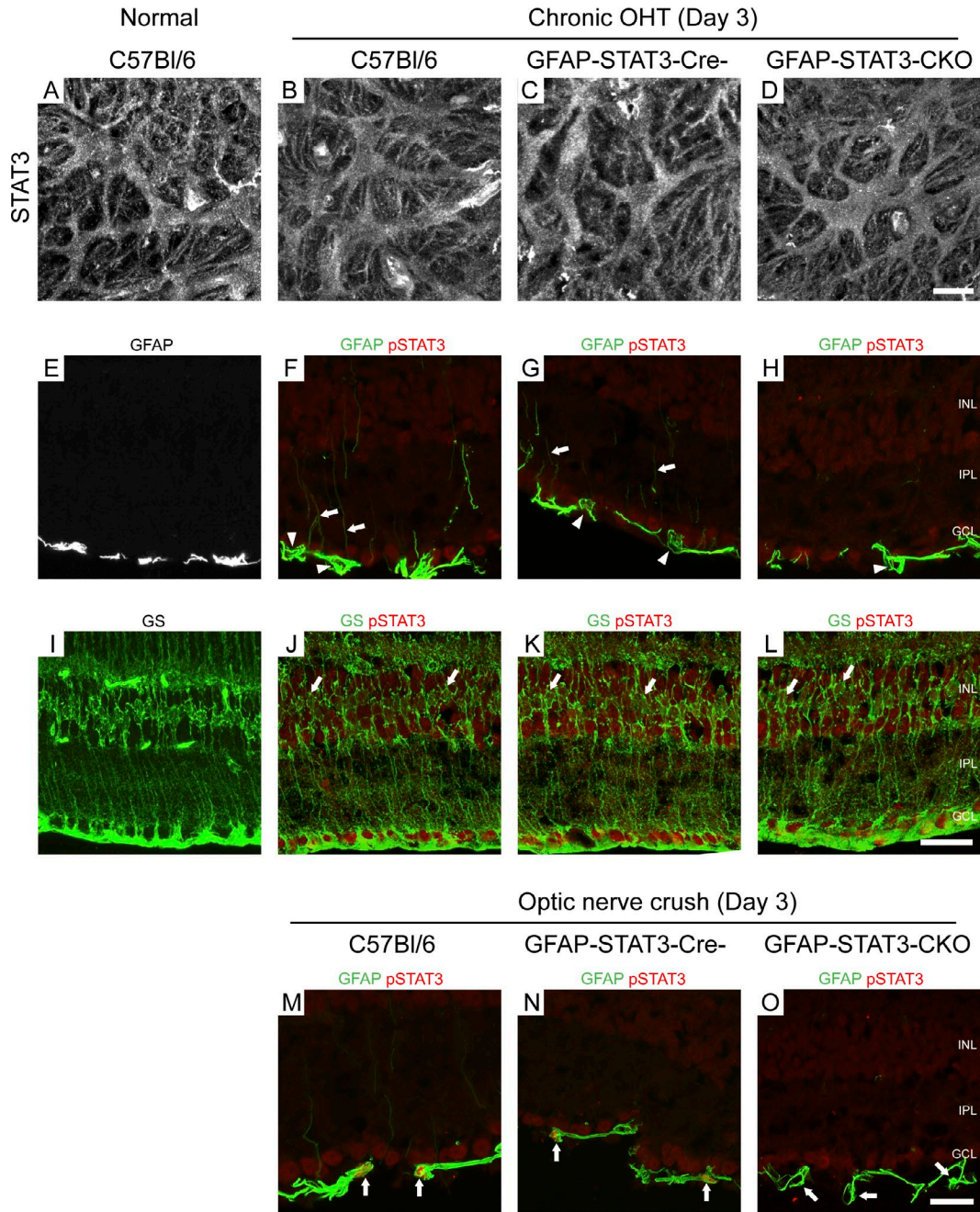


Figure 3. **Immunostaining of STAT3 within the optic nerve head and pSTAT3 within the retina.** (A–D) Transverse cross sections of the glial lamina from normal C57Bl/6 mice and those that underwent chronic OHT immunostained for STAT3. (E–H) Vertical sections of the retina immunostained for either GFAP alone or for GFAP (green) and pSTAT3 (red). Arrows show the GFAP-labeled processes of mildly reactive Müller cells. Arrowheads show the cell bodies of GFAP-labeled astrocytes. (I–L) Vertical sections of the retina immunostained for either glutamine synthetase (GS) alone or for glutamine synthetase (green) and pSTAT3 (red). Arrows show colocalization of glutamine synthetase-labeled Müller cells with pSTAT3. (M–O) Vertical sections of the retina immunostained for GFAP (green) and pSTAT3 (red). Arrows show the cell bodies of GFAP-labeled astrocytes. For all the images, we observed a similar labeling pattern at day 1 (not depicted). GCL, ganglion cell layer; INL, inner nuclear layer; IPL, inner plexiform layer. Each panel represents a typical finding from a sample of three to five mice. Bars: (A–D) 10 μ m; (E–L) 25 μ m; (M–O) 25 μ m.

astrocyte processes and process hypertrophy at day 3 after injury. This time was chosen as we previously performed a time series analysis of GFAP immunostaining (at days 1, 3, and 7)

and determined that the reorganization was most prominent at day 3 after injury (Sun et al., 2010, 2013). We and others have previously shown that GFAP mRNA levels within

the optic nerve head do not change significantly after injury, even after severe injuries such as a nerve crush (Johnson et al., 2007; Qu and Jakobs, 2013; Sun et al., 2013; Choi et al., 2015).

Each of the three injuries induced significant reactive remodeling of astrocytes in the GFAP-STAT3-Cre⁻ and C57BL/6 glial lamina. There was a loss of the large distinct glial tubes and the overall honeycomb arrangement (Fig. 4, A and C–H). However, this remodeling was attenuated in the GFAP-STAT3-CKO mice, where large distinct glial tubes remained and the overall honeycomb arrangement was largely intact (Fig. 4, I–K; dashed ellipses show the glial tubes). Quantification of the remodeling (flooding algorithm; see the Image collection and analysis section of Materials and methods) demonstrated that GFAP-STAT3-CKO mice have 20–30% more process-free area (or black space) compared with the other two mouse strains and across the three injuries, indicating the astrocytes undergo less remodeling (Fig. 4 B and Table S1).

Next, we examined the hypertrophy of astrocyte processes by measuring the width of the thickest GFAP-labeled process at a location of 12–15 μm away from DAPI-labeled nuclei (Sun et al., 2010). Processes in the glial lamina of GFAP-STAT3-Cre⁻ and C57BL/6 mice exhibited significant hypertrophy, showing a 1.5–1.7-times increase in thickness across the three different injury models. This reactive hypertrophy was significantly attenuated in the GFAP-STAT3-CKO mice, the processes displaying a 1.1–1.2-times increase in thickness (Fig. 4 L and Table S1).

Attenuated reactive remodeling in the GFAP-STAT3-CKO glial lamina was associated with greater ganglion cell loss

Next, we wanted to determine whether the diminished astrocyte reactivity within the glial lamina of GFAP-STAT3-CKO mice affected ganglion cell survival. We counted cells in whole mounted retinas that were immunostained with both β III-tubulin, a ganglion cell-specific marker (Chen et al., 2011; Gao and Jakobs, 2016), and DAPI. Counts were performed at a single time point after injury, the earliest time at which we knew from previous studies there would be sufficient ganglion cell loss to see an effect from the *STAT3* KO. Ganglion cells degenerate rapidly after an optic nerve crush (within 3–7 d depending on the duration of the crush; Li et al., 1999; McKinnon et al., 2009; Ryu et al., 2012; Liu et al., 2014; Choudhury et al., 2015), and we chose to perform our counts at day 3 after crush. In contrast, ganglion cell degeneration in the chronic OHT model is much slower, and we counted cells at day 30, a time point also used by numerous other studies (Sappington et al., 2010; Chen et al., 2011; Della Santina et al., 2013; Gao and Jakobs, 2016). For the transient OHT model, we chose an endpoint time of 14 d based on our previous study (Sun et al., 2013). GFAP-STAT3-CKO mice showed a preferential loss of ganglion cells after each of the injuries, losing 20–30% more ganglion cells compared with their control strain and C57BL/6 mice (Fig. 5 A and Table S2).

We confirmed ganglion cell loss by counting surviving axons from paraphenylenediamine (PPD)-stained cross sections of the optic nerves (see the Electron microscopy and quantification of axon loss with PPD stain section of Materials and methods). PPD darkly stains damaged axons allowing for sensitive detection of injury (Fig. 5, B and C, arrows). We found that, at day 14 after transient OHT, GFAP-STAT3-CKO mice showed a significantly greater amount of ganglion cell loss compared with axon loss ($P < 0.01$; Student's *t* test; Fig. 5, A and D; and Table S2). However, there was no significant difference when we made this comparison with the other two mouse strains. At day 30 after chronic OHT, there was no significant difference between ganglion cell loss and axon loss for any of the mouse strains ($P > 0.1$; Student's *t* test; Fig. 5, A and F; and Table S2). Our counts here were performed late after the onset of injury, and we cannot speak to whether there was an early preferential loss of axons compared with ganglion cell soma, as has been shown to occur in glaucomatous neurodegeneration (Howell et al., 2007). We also noted that there was no difference in the cross-sectional area of the optic nerve for any of the mouse strains after both transient and chronic OHT (Fig. 5, E and G). Because of the severe nature of an optic nerve crush injury, we did not examine the nerves with PPD.

Attenuated reactive remodeling in the GFAP-STAT3-CKO glial lamina was associated with greater visual function loss

To evaluate the effect of knocking out *STAT3* on visual function after injury, we assessed the full-field dark-adapted ERG and the optomotor response. Ganglion cell function was assessed by measuring the positive scotopic threshold response (STR [pSTR]), a component of the ERG most sensitive to IOP elevations in both mice and rats (Fortune et al., 2004; Bui et al., 2005; He et al., 2006; Holcombe et al., 2008; Kong et al., 2009; Frankfort et al., 2013; Pérez de Lara et al., 2014; Porciatti, 2015). Consistent with the greater ganglion cell loss, GFAP-STAT3-CKO mice showed the greatest reduction in pSTR amplitude across the different injuries (Figs. 6 and 7). By day 30, these mice showed a 20–30% greater reduction in amplitude compared with the other two strains (Fig. 7 D). There was no significant difference in the reduction in pSTR amplitude between GFAP-STAT3-Cre⁻ and C57BL/6 mice for any of the injuries or times. Outer retinal function was assessed using the scotopic a- and b-wave amplitude. As expected, both waveforms were not as affected by injury as the inner retina-derived pSTR. Although injury induced a small decrease in the a- and b-wave amplitude over time, there was no significant difference in this decrease between the mouse strains for each of the injuries (Fig. 8).

Similar to their ERG response, GFAP-STAT3-CKO mice demonstrated a preferential reduction in spatial frequency thresholds that was most evident after chronic OHT (Fig. 9). The treated right eye of GFAP-STAT3-CKO mice showed a significantly greater reduction than the right eye of its control strain from day 3 onwards (Fig. 9 A). By day

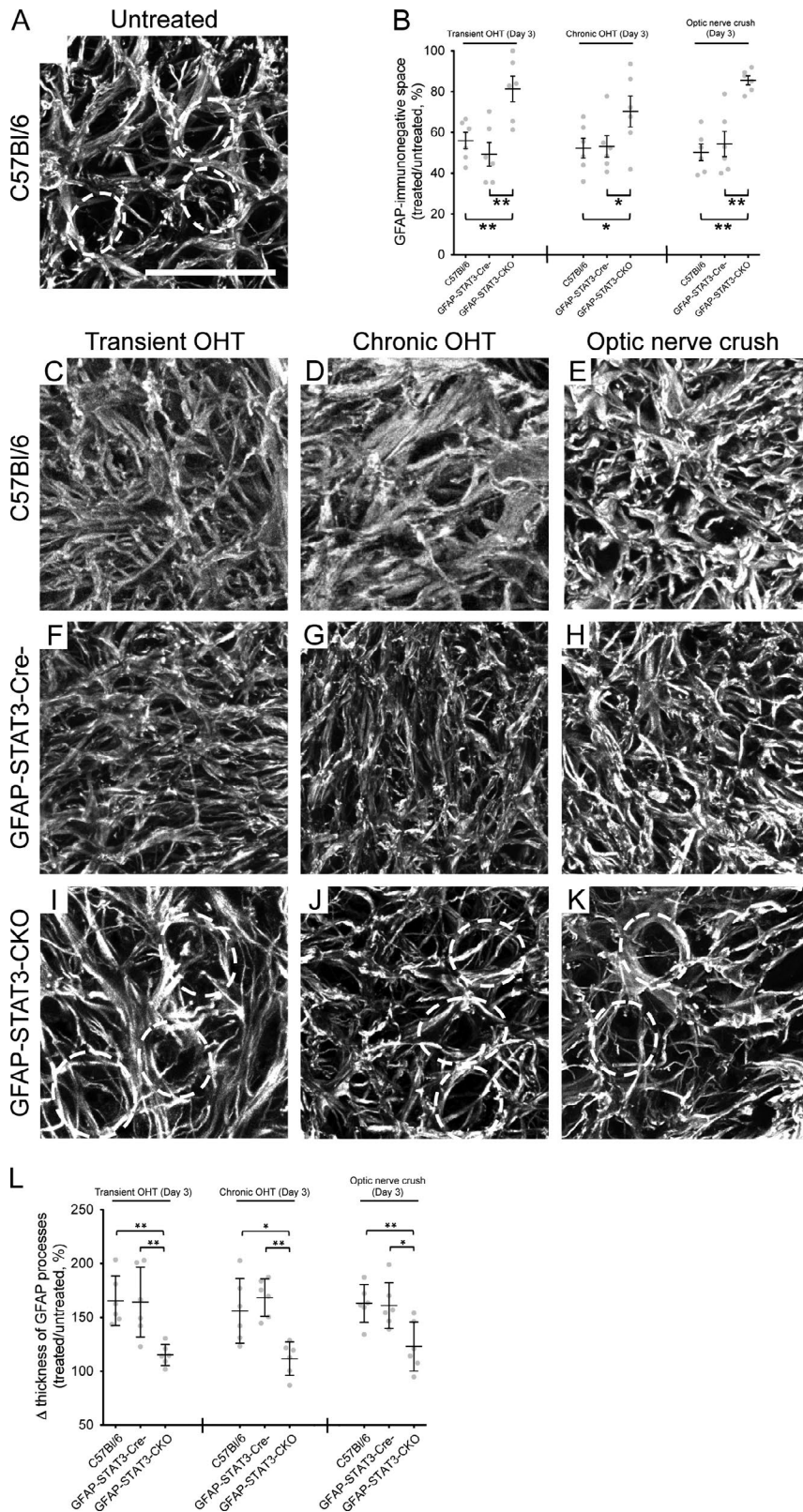


Figure 4. STAT3 KO mice show attenuated astrocyte reactivity and remodeling after injury. (A) A transverse section of the glial lamina from normal C57Bl/6 mice immunostained for GFAP. (B) Changes in the amount of GFAP immunonegative space within the glial lamina across the various mouse strains and injury models. (C–K) Transverse sections of the glial lamina immunostained for GFAP. (L) A comparison of the change in the thickness of GFAP-labeled processes within the glial lamina across the various mouse strains and injury models. (B and L) See Table S1 for the absolute numbers. Also, we are not making comparisons across injury models but, rather, between strains within each injury model. In all cases, there were no statistical differences between GFAP-STAT3-Cre⁻ and C57Bl/6 mice. Each gray dot represents an individual mouse ($n = 6$ for each group), and for each mouse in L, processes from 10–15 astrocytes were averaged. Horizontal lines represent the group means and SD. One-way ANOVA with Tukey posttest was used. *, $P < 0.05$; **, $P < 0.01$. (A and C–K) Each image represents a typical finding from a sample of six mice. The dashed ellipses indicate the distinct glial tubes. Bar, 20 μm .

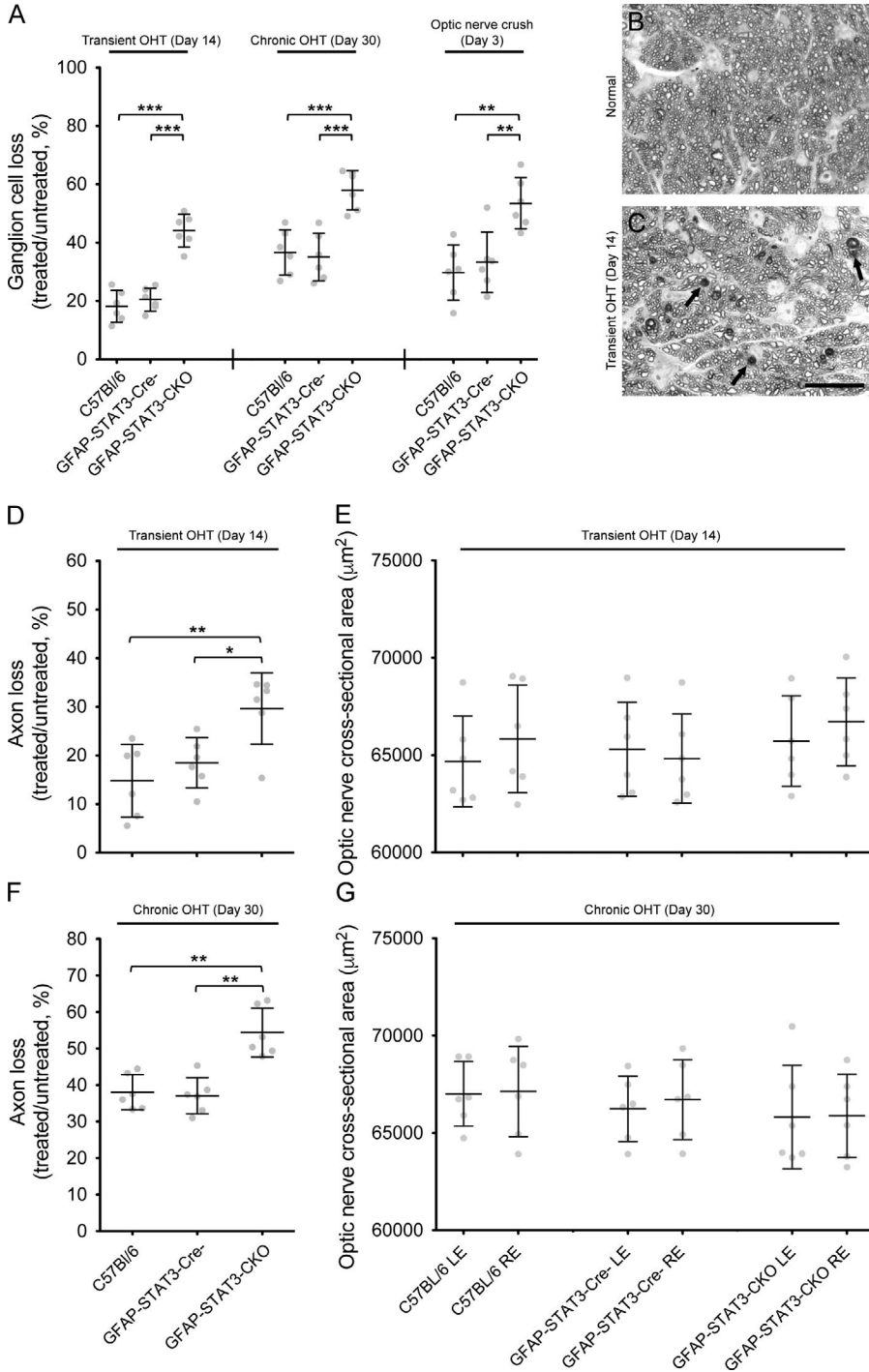


Figure 5. Ganglion cell soma and axon loss in the different mouse strains after transient and chronic OHT. (A) Ganglion cell loss in the treated eye, as a percentage of the untreated contralateral eye, across the various mouse strains and injury models. We are not making comparisons across injury models but, rather, between strains within each injury model. In all cases, there were no statistical differences between GFAP-STAT3-Cre⁻ and C57Bl/6 mice. (B and C) A representative PPD-stained cross section of normal (B) and injured (C) optic nerve from GFAP-STAT3-CKO mice. Damaged axons show a major loss of the normal axon profile, as well as clumps of myelin debris. These axons stain darkly with PPD (C, arrows). Bar, 20 µm. (D–G) Axon loss in the treated eye as a percentage of the untreated contralateral eye for each mouse strain after transient (D) and chronic (F) OHT and the changes in the optic nerve cross-sectional area (E and G). There was no significant difference in the cross-sectional area of the optic nerve for the different mouse strains after both injuries. Each gray dot represents an individual mouse (*n* = 6 for each group). Horizontal lines represent the group means and SD. See Table S2 for the absolute numbers. LE, left eye; RE, right eye. One-way ANOVA with Tukey posttest was used. *, *P* < 0.05; **, *P* < 0.01; ***, *P* < 0.001.

30, thresholds were reduced to 0.16 ± 0.03 cycles/degree compared with 0.32 ± 0.03 cycles/degree in the control strain (*P* < 0.001). Thresholds were not as greatly reduced after transient OHT (Fig. 9 B), where a significant difference was first observed at day 14 and thresholds were reduced to 0.31 ± 0.05 cycles/degree. Because of the severe nature of a nerve crush, optomotor responses were completely abolished in the treated right eye of all the mouse strains from as

early as day 3 after crush (Fig. 9 C). Thresholds were affected neither in the untreated left eyes of any mouse strain nor after any of the injuries.

DISCUSSION

Although it is well accepted that optic nerve head astrocytes undergo significant reactive remodeling in glaucoma, its mechanism, function, and effect on visual function are not

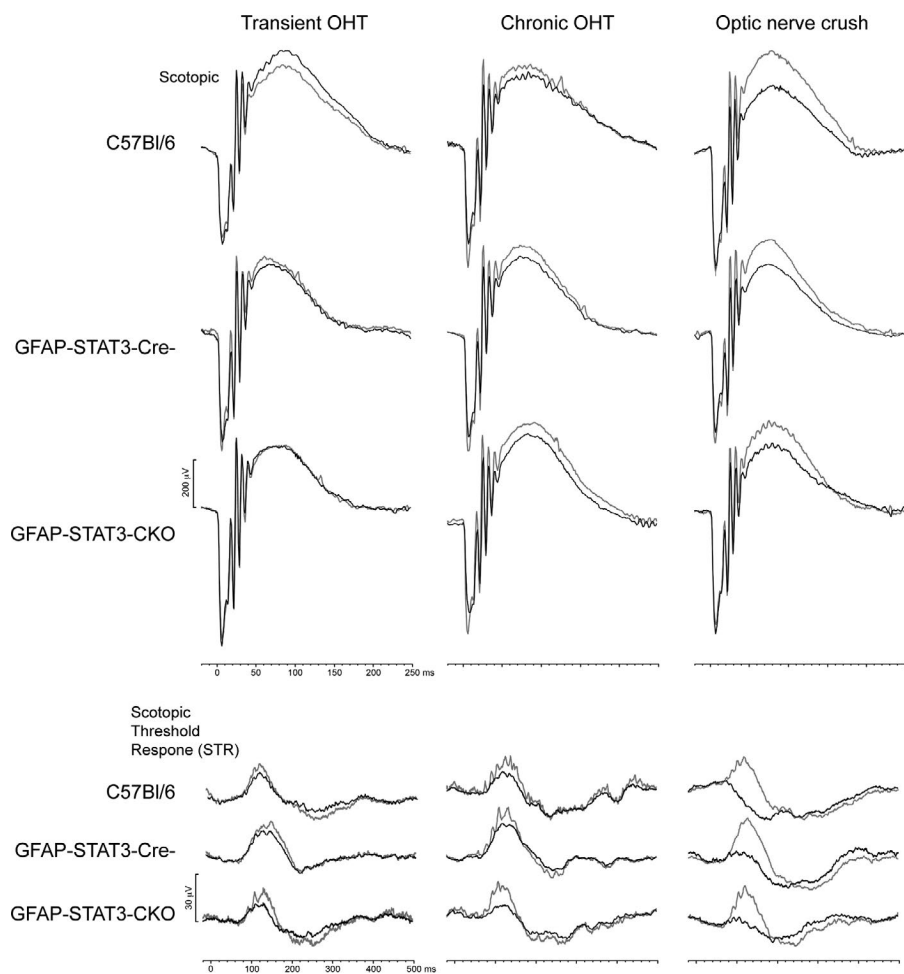


Figure 6. **Representative ERG responses from the various mouse strains at day 30 after injury.** Responses from the untreated left eye are in gray, and the treated right eye is in black. Outer retinal function is represented by the scotopic waveforms and inner retinal function by the STR. Scotopic responses were obtained using a single-flash intensity of 2.13 log cd.s.m⁻², and STRs were obtained using a single-flash intensity of -5.00 log cd.s.m⁻². Each waveform represents a typical finding from a sample of six mice.

well studied. Is it a beneficial or harmful response for visual outcome? Here, we report that the STAT3 signaling pathway is an important mediator of astrocyte reactivity in the glaucomatous optic nerve head, playing an important role in astrocyte hypertrophy and in the formation of a glial scar. Astrocyte reactivity is beneficial, as attenuating reactivity in injured mice leads to increased ganglion cell and visual function loss.

Chronic OHT induces reactive changes in the glial lamina more than the retina

In GFAP-STAT3-Cre⁻ and C57BL/6 mice subjected to chronic OHT, pSTAT3 was up-regulated early in reactive astrocytes within the glial lamina (days 1 and 3). Retinal astrocytes at this time did not show an up-regulation of pSTAT3 and were not highly reactive. Therefore, the KO of STAT3 would have little effect on retinal astrocytes. In contrast, Müller cells showed a low-level up-regulation of pSTAT3 and some reactivity; we observed a few processes with increased GFAP immunoreactivity. These findings suggest that chronic OHT induces distinct reactive changes primarily in the glial lamina. The deleterious effects on visual function that we observed in the STAT3 KO animals are therefore

likely caused by the inhibition of astrocyte reactivity in the glial lamina rather than the retina.

STAT3 signaling and its role in reactive astrocytes

STAT3 is involved in many cellular processes, not only with those directly related to the classical reactive phenotype such as structural remodeling, proliferation, and migration, but also with processes hypothesized to be important for the pathophysiology of glaucoma, such as inflammation and deprivation of growth factors.

For example, inhibiting or knocking out STAT3 attenuated the increase in GFAP mRNA and/or protein levels in reactive astrocytes. Levels of GFAP are also reduced by STAT3 inhibition in untreated animals, suggesting that STAT3 controls the basal expression of GFAP (Herrmann et al., 2008; Wanner et al., 2013; Levine et al., 2016). Evidence for the involvement of STAT3 in astrocyte proliferation is indirect. JAK inhibitors reduce the number of proliferating reactive astrocytes after spinal cord injury (Tsuda et al., 2011), and the formation of the glial scar, which is composed of newly proliferated astrocytes, is also altered in STAT3 KO mice (Wanner et al., 2013; Anderson et al., 2016). STAT3 KO reduces the

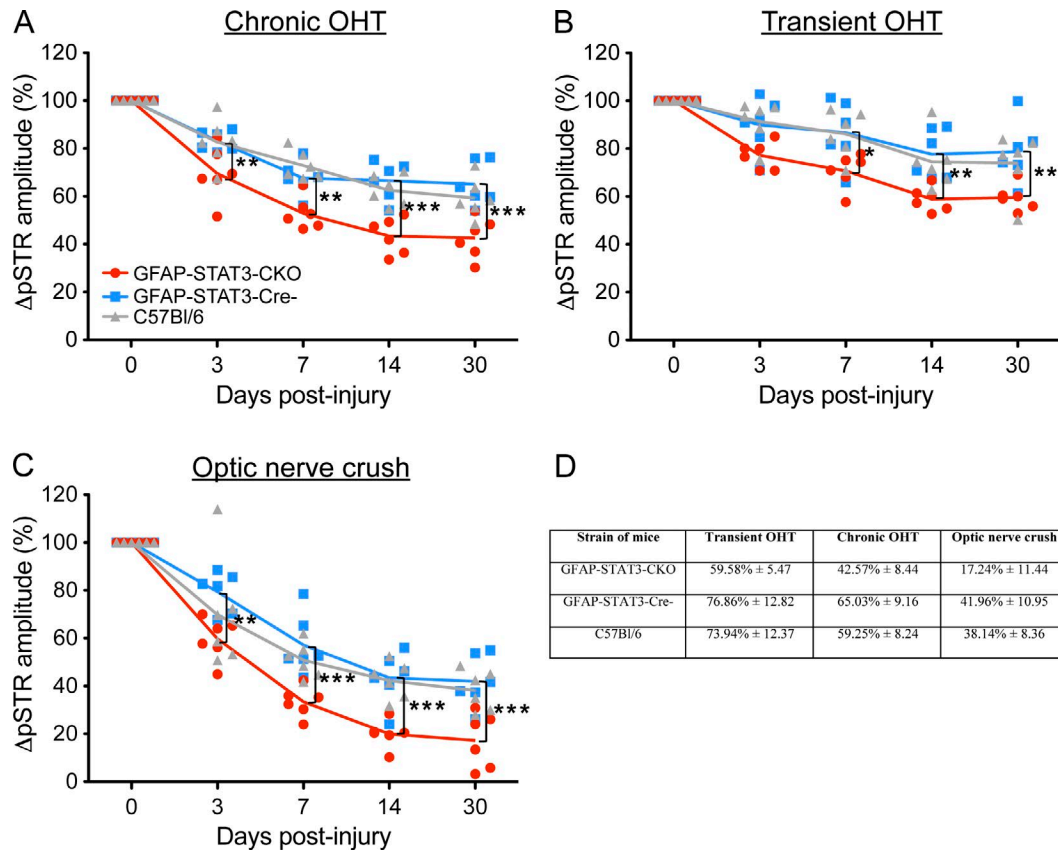


Figure 7. Changes in the pSTR amplitudes after injury. (A–D) A single-flash intensity of -5.00 log cd.s.m⁻² was used to measure pSTR. The actual percentage value for the pSTR amplitude at day 30 is tabulated in D, where values are mean ± SD. A two-way repeated-measures ANOVA with Bonferroni posttest for three selected comparisons was performed (GFAP-STAT3-CKO vs. GFAP-STAT3-Cre⁻, GFAP-STAT3-CKO vs. C57Bl/6, and GFAP-STAT3-Cre⁻ vs. C57Bl/6). Here, we only show the statistical differences between the GFAP-STAT3-CKO mice and its control strain (GFAP-STAT3-Cre⁻). There was no significant difference between GFAP-STAT3-Cre⁻ and C57Bl/6 mice for any injury and for any times after injury. Changes in the pSTR amplitude were calculated from the same eye before and after injury (e.g., amplitude after injury/amplitude before injury × 100%). Each colored dot represents an individual mouse ($n = 6$ for each mouse strain in each injury model). *, $P < 0.05$; **, $P < 0.01$; ***, $P < 0.001$.

migration of reactive astrocytes after in vitro scratch injury (Okada et al., 2006), and STAT3 regulates the transcription of genes implicated in matrix remodeling and cell adhesion proteins (Gao and Bromberg, 2006). During glial scar formation, reactive astrocyte processes reorient themselves to enclose immune cells and fibroblasts. This organization is disrupted in STAT3 KO mice (Wanner et al., 2013).

With regards to inflammation, STAT3 in astrocytes regulates the production of cytokines and chemokines during reactivity. Inhibition of the STAT3 pathway in astrocytes reduced mRNA levels of IL-6, IL1 β , IL-4, and vascular endothelial growth factor (Wang et al., 2012b). Intrathecal injection of the STAT3 inhibitor Stattic in an LPS model of inflammation reduced the astrocytic expression of Ccl20, Cx3cl1, Cxcl5, and Cxcl10 (Liu et al., 2013). Lipocalin 2, a protein highly expressed by reactive astrocytes (Zamanian et al., 2012), may serve as an inflammatory mediator, and its production by reactive astrocytes is dependent on STAT3 (Shiratori-Hayashi et al., 2015). Factors released by reactive

astrocytes in a STAT3-dependent manner may also affect microglial reactivity and modulate their activity (Nobuta et al., 2012; Ben Haim et al., 2015; Hristova et al., 2016).

We report in this study that inhibiting astrocyte reactivity led to a greater loss of ganglion cells and visual function. The most parsimonious explanation—and the one we favor—would be that astrocyte reactivity is protective of ganglion cell axons, and therefore, interfering with the reactive process leads to a more severe phenotype. However, our results should be interpreted with caution. First, we cannot exclude the possibility that knocking out STAT3 also affects constitutive pathways unrelated to reactivity, causing the beneficial phenotype we observed. Second, though STAT3 is a key regulator, multiple other pathways may also be associated with reactivity. NF- κ B, endothelin-1, JNK/c-Jun, CEPB1, EphB2, Nrf2, and SOCS3 can also play a role in mediating various aspects of reactivity, including up-regulation of structural molecules, hypertrophy, proliferation, migration, scar formation, and antiinflammatory effects (Sofroniew, 2009).

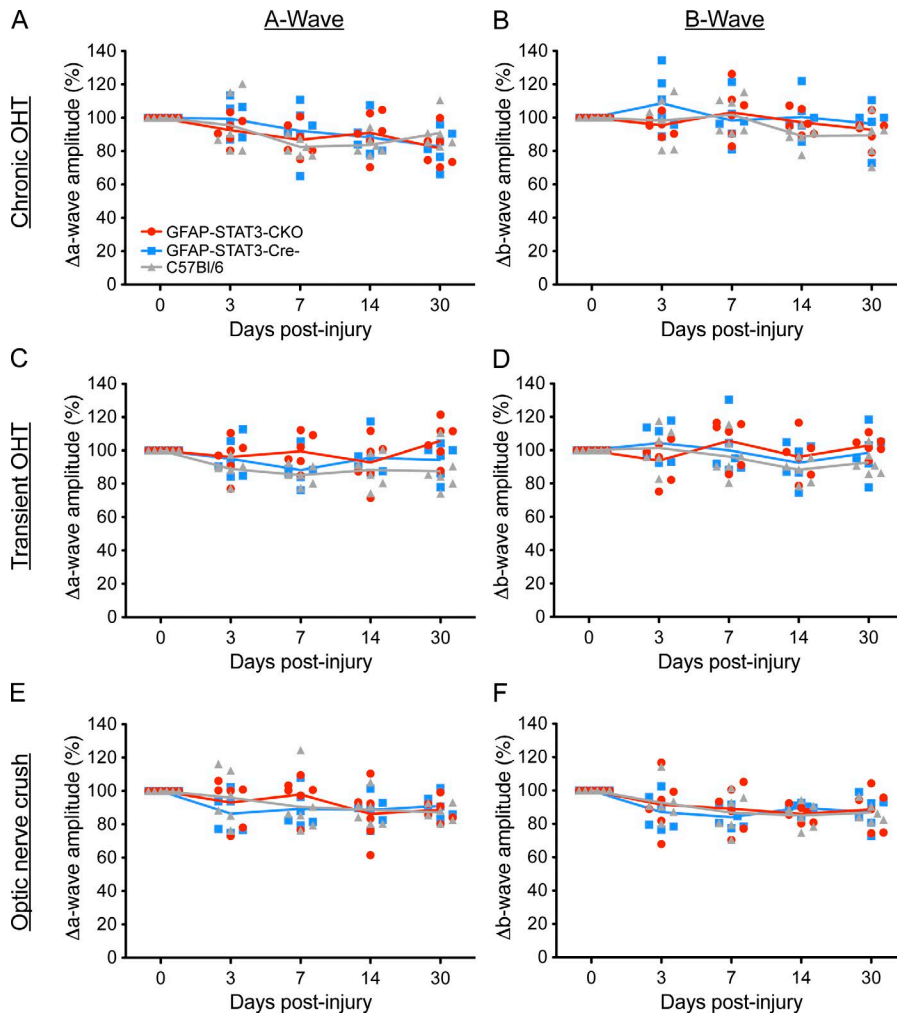


Figure 8. **Changes in the scotopic a- and b-wave amplitudes after injury.** (A–F) A single-flash intensity of 2.13 log cd.s.m⁻² was used to measure the a- and b-wave. A two-way repeated-measures ANOVA with Bonferroni posttest for three selected comparisons was performed (GFAP-STAT3-CKO vs. GFAP-STAT3-Cre⁻, GFAP-STAT3-CKO vs. C57BL/6, and GFAP-STAT3-Cre⁻ vs. C57BL/6). There was no significant difference between the mouse strains for each of the injuries. Changes in the a- and b-wave amplitude were calculated from the same eye before and after injury (e.g., amplitude after injury/amplitude before injury × 100%). Each colored dot represents an individual mouse (*n* = 6 for each mouse strain in each injury model).

The fact that knocking out *STAT3* did not completely prevent process hypertrophy and remodeling does indeed suggest that other pathways are involved.

Transient episodes of pressure-related stress can induce long-term damage

The transient OHT model helps us to understand processes that are relevant to the early stages of glaucoma because it mimics the cycles of relatively mild increases in pressure to which the optic nerve head is repeatedly exposed (Li and Liu, 2008; Downs et al., 2011; Crowston et al., 2015). An interesting finding from this study was that a single transient elevation of IOP to 30 mmHg for 2 h induced long-term histological and functional damage. In a previous study, we elevated the IOP to 30 mmHg for 1 h and did not observe gross degeneration of the axons, albeit axon or ganglion cell loss was not quantified and the ERG response was not examined (Sun et al., 2013). A study by Kong et al. (2009) examined the long-term effects of a single transient elevation of IOP on the ERG components and found a similar result to our current study. 7 d after a single elevation of the IOP to 50 mmHg for 30 min, there was a per-

sistent reduction in the pSTR amplitude of 30%. Crowston et al. (2015) found a similar degree of functional degeneration, although in both these studies, ganglion cell loss was not assessed. He et al. (2006) suggested that the IOP integral (e.g., 50 mmHg × 30 min = 1,500) is an important predictor of retinal dysfunction, so it is not surprising that in our current study, which has an IOP integral of 3,600 (30 mmHg × 120 min), we saw persistent histological and functional deficits even at day 14 after injury. The capacity to recover after transient OHT depends on the magnitude and duration of the elevation, and both factors collectively define a threshold for permanent damage (He et al., 2006; Kong et al., 2009; Bui et al., 2013). It may be that by increasing the duration of the IOP elevation from 1 to 2 h a critical threshold at which full recovery is possible has been passed. These results suggest that a single episode of pressure-related stress can produce long-term damage; a chronic elevation in IOP may not be required to cause irreversible losses.

Beneficial functions of reactive astrocytes

Astrocytes respond to virtually all CNS injuries and diseases by becoming reactive. This is not a single all-or-none

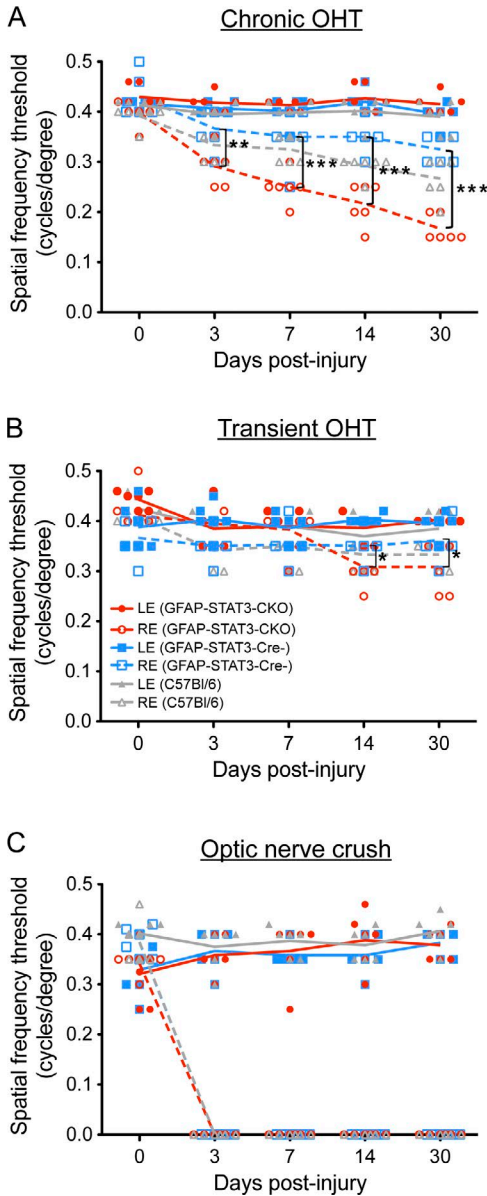


Figure 9. Changes in spatial frequency threshold after injury. (A–C) Each panel shows the treated right eye (RE; dashed colored lines) and untreated left eye (LE; solid colored lines). A two-way repeated-measures ANOVA with Bonferroni posttest for three selected comparisons was performed (GFAP-STAT3-CKO vs. GFAP-STAT3-Cre⁻, GFAP-STAT3-CKO vs. C57Bl/6, and GFAP-STAT3-Cre⁻ vs. C57Bl/6). There was no significant difference between any of the untreated left eyes of any mouse strains in any of the injuries. Each colored dot represents an individual mouse ($n = 6$ for each mouse strain in each injury model). *, $P < 0.05$; **, $P < 0.01$; ***, $P < 0.001$.

response but a complex, heterogeneous process controlled in a context-dependent manner by a multitude of signaling mechanisms. In line with this complexity, reactive astrocytes are attributed to have both beneficial and detrimental effects (Sofroniew and Vinters, 2010). In the brain and spinal cord, studies across various injury models (e.g., acute traumatic

injury, stroke, inflammation, and neurodegenerative diseases) have largely concluded that the reactive process, at least in its early stages, is adaptive and beneficial—that various functions of reactive astrocytes are normal and indeed essential for the proper recovery of tissue.

Numerous *in vivo* transgenic loss-of-function studies provide evidence that gene deletion or KO of molecules, such as *STAT3*, from astrocytes or ablation of reactive astrocytes leads to increased lesion size, exacerbates the spread of and prolongs the inflammatory response, increases neuronal loss and demyelination, and eventually impairs functional recovery (Bush et al., 1999; Faulkner et al., 2004; Brambilla et al., 2005; Myer et al., 2006; Okada et al., 2006; Herrmann et al., 2008; Li et al., 2008; Voskuhl et al., 2009; Wanner et al., 2013). In contrast, hastening the development of astrocyte reactivity by knocking out suppressor of cytokine signaling 3 (*SOCS3*; the negative feedback molecule of *STAT3*) improved compaction of the lesion site and functional recovery (Okada et al., 2006). A recent study by Wong et al. (2015) subjected rats to transient OHT. In common with our results and the studies in the CNS just mentioned, they found that *STAT3* was activated early after injury and that inhibiting its activation reduced astrocyte reactivity; however, this inhibition was associated with an improved ganglion cell survival, although the improvement was marginal. Furthermore, cell counts were performed only on hematoxylin and eosin–stained material and included all cells in the ganglion cell layer, of which 59% are not ganglion cells but are displaced amacrine cells (Jeon et al., 1998). Our results here are consistent with the findings in the brain and spinal cord: that reactivity is beneficial and, if prevented, results in a greater ganglion cell and functional loss.

Axon–astrocyte relationship within the optic nerve head

What is the communication between the axons and astrocytes in the lamina region? Are the axons injured first, which in turn send extracellular distress signals to the astrocytes instructing them to become reactive, do the astrocytes respond first and then affect the axons, or do both occur simultaneously? In the first case, an increase in IOP could cause a subthreshold insult to the axons (Quigley, 1999; Buckingham et al., 2008). Although axons are capable of sustaining minor membrane deformations, they are relatively rigid structures within an elastic extracellular surround (Javid et al., 2014), and deleterious mechanical stress experienced by IOP rises could induce plasmalemmal instability and cytoskeletal disassembly (Pettus and Povolishock, 1996; Singleton and Povolishock, 2004). ATP has been suggested as one such signaling molecule (Ahmed et al., 2000; Verderio and Matteoli, 2001; Neary et al., 2003, 2005); it can be released from axons of the white matter (Fields and Stevens, 2000; Hamilton et al., 2008; Fields and Ni, 2010). In the second case, astrocytes could respond directly to the pressure by membrane stretching or distortions. Astrocytes, including those in the optic nerve head, express mechanosensitive ion channels as well as nontraditional, stretch-sensitive cation channels (Bowman et al., 1992; Islas

et al., 1993; Choi et al., 2015). Such stretch injury can lead to the secretion of ATP or vasoactive molecules such as endothelin-1 and isoprostanes, as well as inositol triphosphate and matrix metalloproteinase 9 (Rzigalinski et al., 1997; Hoffman et al., 2000; Ostrow et al., 2011; Ralay Ranaivo et al., 2011; Pan et al., 2012). These diverse effects could have a wide variety of consequences that impact neighboring astrocytes and axons. For example, ATP is known to induce a rapid rise in $[Ca^{2+}]_i$ in reactive astrocyte networks, which precede polarization of the astrocyte processes toward the site of injury and recruitment of microglia and neutrophils (Davalos et al., 2005; Kim and Dustin, 2006; Roth et al., 2014).

Does up-regulation of *STAT3* and the associated reactivity suggest a path toward a glaucoma therapy? Long-term constitutive activation of *STAT3* (e.g., the phosphorylation of *STAT3*) is abnormal and highly oncogenic; the *STAT3* pathway contributes to tumor cell proliferation and survival and maintaining an inflammatory environment (Yu and Jove, 2004; Wang et al., 2012a). However, in vivo and in vitro activation of *STAT3* by the pharmacological agent colivelin resulted in a neuroprotective effect against Alzheimer's disease and amyotrophic lateral sclerosis-related toxicity, with no reported effects of inflammation or glioma development (Chiba et al., 2005; Matsuoka et al., 2006; Wu et al., 2015). An important first step might be determining a potential short-term therapeutic window, i.e., an appropriate time and duration for *STAT3* activation.

MATERIALS AND METHODS

Animals

All experiments with animals were approved by the Institutional Animal Care and Use Committee of Massachusetts Eye and Ear Infirmary. Male mice age 2–3 mo were housed in a 12-h light/dark cycle and received food and water ad libitum. Three mouse strains were used in this study: (1) wild-type C57BL/6 (stock no. 000664; The Jackson Laboratory), (2) an astrocyte-specific *STAT3* CKO strain, referred to as GFAP-*STAT3*-CKO, and (3) mice homozygous for *STAT3-loxP* but without the *GFAP-Cre* transgene, referred to as GFAP-*STAT3*-*Cre*⁻. This third strain served as a control to the GFAP-*STAT3*-CKO strain of mice. Both the *STAT3-loxP* and *GFAP-Cre* mice are on C57BL/6 backgrounds, and so, we have included these mice in this study.

To generate the *STAT3* CKO line (GFAP-*STAT3*-CKO), mice heterozygous for *GFAP-Cre* (B6.Cg-Tg[GFAP-cre]73.12Mvs/J; stock no. 012886; The Jackson Laboratory) were crossed to mice homozygous for *STAT3-loxP*, which has exon 22 of the *STAT3* gene flanked by *loxP* sites (Takeda et al., 1998; Herrmann et al., 2008). Exon 22 is a region necessary for *STAT3* activation. M. Sofroniew (University of California, Los Angeles, Los Angeles, CA) provided the *STAT3-loxP* mice. GFAP-*STAT3*-CKO mice developed and thrived in a manner indistinguishable from their control strain and C57BL/6 mice. They appeared normal in size and did not display any gross physical or behavioral abnormalities. Astrocytes in the white

and gray matter were similar in size, shape, overall appearance, and density in both control and the *STAT3* KO mice (Herrmann et al., 2008). We also found that there was no difference in the general cytoarchitecture of the optic nerve and retina and the appearance of the astrocytes between the control and *STAT3* KO mice. To test the specificity of *Cre* targeting to astrocytes in the retina and optic nerve, *GFAP-Cre* mice were crossed to a reporter strain that expressed tdTomato downstream from *loxP*-flanked stop signals via the *ROSA* promoter (B6;129S4-Socs3^{tm1AyoS}/J; stock no. 023035; The Jackson Laboratory). In the offspring, tdTomato colocalized with established astrocyte-specific markers GFAP, S100 β , and vimentin (Fig. S3).

Tissue preparation

Animals were anesthetized with an intraperitoneal injection of 100 mg/ml ketamine and 20 mg/ml xylazine and, when required, euthanized by carbon dioxide overdose. The skull was opened, and the brain was carefully removed to expose the optic nerve and chiasm. The head of the animal was fixed in 4% paraformaldehyde for 4 h at 4°C and then rinsed in PBS (3 \times 5 min). Procedures for dissecting the optic nerve and retina have been previously described (Sun et al., 2009, 2010). The optic nerve was cryoprotected overnight in 30% sucrose at 4°C, mounted in freezing medium, and sectioned at 14- μ m thickness. Sections were collected on coated slides and either stored at -20°C or used immediately. Retinas were stored in PBS at 4°C until needed.

Immunohistochemistry

Optic nerve sections or whole retinas were washed in PBS (3 \times 5 min) and then incubated in blocking solution (5% donkey serum, 0.5% Triton X-100, and 1% bovine serum albumin in PBS) for 1 h at room temperature (RT), followed by incubation in primary antibodies either overnight (optic nerves) or for 3–5 d (retinas), always at 4°C. The primary antibodies used were: rabbit anti-GFAP (1:2,000; Abcam), mouse anti-SMI32 (1:400; Covance), rabbit anti-S100 β (1:200; Abcam), mouse anti-vimentin (1:100; Abcam), rabbit anti- β III-tubulin (1:200; Cell Signaling Technology), mouse anti-GFAP (1:400; Sigma-Aldrich), mouse anti-pSTAT3 (1:100; Cell Signaling Technology), and mouse anti-*STAT3* (1:2,000; Cell Signaling Technology). The next day, tissue were washed in PBS (3 \times 5 min) and incubated with secondary antibodies conjugated to rhodamine (1:200; donkey anti-rabbit; Jackson ImmunoResearch Laboratories, Inc.) or FITC (1:400; donkey anti-mouse; Jackson ImmunoResearch Laboratories, Inc.) for 2 h (optic nerves) or 3 d (retinas) at RT. Optic nerve sections were washed in PBS (3 \times 5 min) and mounted in ProLong Gold Antifade medium (Thermo Fisher Scientific). Retinas were incubated with the nuclear dye DAPI for 20 min, washed in PBS (3 \times 5 min), and mounted in Vectashield (Vector Laboratories).

Image collection and analysis

Images were acquired on a laser scanning confocal microscope (TCS SP5; Leica Biosystems) and then exported into ImageJ

(National Institutes of Health). All fluorescent images are maximum intensity projections (step size 0.3–0.4 μm), and all the image panels in a single figure contain projections made from the same number of image stacks. The brightness and contrast of the final images were adjusted using Photoshop CS4 (Adobe); no other digital image processing was performed.

A user-written Image J plug-in was developed to quantify the change in astrocyte remodeling within the glial lamina based on the GFAP labeling pattern (Sun et al., 2013). In the normal glial lamina, the center of each glial tube contains fewer processes and more black space (Fig. 1), and thus, every single black pixel within the tube is surrounded by many other black pixels. Reactive remodeling disrupts the honeycomb/glial tube architecture, and astrocyte processes fill in the glial tubes, reducing the amount of process-free area and overall the amount of black space within the glial lamina (Fig. 4). To quantify this remodeling, the algorithm line-scans an image and measures the number of black pixels surrounding each single pixel of the image (Sun et al., 2013). This process is sometimes referred to as a flooding measurement, as though the center pixel were a point source from which fluid flows until it meets a barrier. The lumen of a blood vessel was used to determine the black point, and this was taken as a reference point for each image. The sizes of the black areas were converted from a pixel count to microns squared and then presented as a percentage of the control.

Electron microscopy and quantification of axon loss with PPD stain

Optic nerves were fixed with half-strength Karnovsky's fixative (2% formaldehyde/2.5% glutaraldehyde in 0.1 M sodium cacodylate buffer, pH 7.4; Electron Microscopy Sciences) for a minimum of 12 h at 4°C. Then, tissue was rinsed in 0.1 M sodium cacodylate buffer, postfixed with 2% osmium tetroxide in 0.1 M sodium cacodylate buffer, and en bloc stained with 2% aqueous uranyl acetate. Then, the tissue was dehydrated with graded ethyl alcohol solutions, transitioned with propylene oxide, resin infiltrated in tEPON-812 epoxy resin (Tousimis), and polymerized in silicone molds at 60°C. Ultrathin sections were cut at 70–90-nm thickness from the epoxy block using an EM UC7 ultramicrotome (Leica Biosystems) and a diamond knife and then collected onto grids stained with aqueous 2% uranyl acetate and Sato's Lead citrate. Grids were imaged using a transmission electron microscope (Tecnai G2 Spirit; Thermo Fisher Scientific) at 80 kV interfaced with a digital charge-coupled device camera (AMT XR41; Advanced Microscopy Techniques) for digital TIFF file image acquisition.

PPD differentially stains damaged axons, allowing for sensitive detection of axon injury (Howell et al., 2007; Gao and Jakobs, 2016). Semi-thin sections were cut at 1 μm with a diamond knife on the UC7 ultramicrotome, collected on slides, and then dried on a slide warmer. Slides were stained with 2% aqueous PPD solution (MP Biomedicals) for 30 min at RT, rinsed, air dried, and then mounted and cover-slipped.

Axon loss was determined from PPD-stained optic nerve cross sections. Six rectangular regions from each section were photographed at a magnification of 100 ($87 \times 65 \mu\text{m}^2$). Axons were counted using the threshold and analyze particles functions of Image J. Damaged axons stain darkly with PPD and are not counted. Using this automated method, we found that the number of axons counted was within 7% of the number determined manually by four independent observers blind to the genotype of the animal and the experimental condition. Axonal densities per optic nerve were calculated by averaging the data from the six regions. The percentage of axon loss was calculated as the number of axons in the treated eye divided by the number in the untreated eye. The area of the optic nerve cross section was determined three times by outlining its outer border using Image J and then averaged. Axon counts were performed by individuals blinded to the genotype of the animals and the injury induced.

Transient OHT

Using a micromanipulator, the tip of a glass microneedle (50 μm) is inserted into the anterior chamber through the center of the cornea. The needle is connected to a pressure transducer, which is in series with a sterile saline bag, the height of which determines the hydrostatic pressure delivered to the eye (John et al., 1997; Kong et al., 2009; Sun et al., 2013; Crowston et al., 2015). Pressure transducer calibration was performed by referencing to a sphygmomanometer. Based on the normal mouse IOP, our previous results, and the levels to which IOP is typically elevated in other experimental models (increased to 23–30 mmHg, including in a model of hereditary glaucoma), the IOP was raised to 30 mmHg for 2 h (John et al., 1998; Libby et al., 2005; Saleh et al., 2007; Kong et al., 2009; Sun et al., 2013). This level of IOP elevation does not cause ischemia (Sun et al., 2013).

Chronic OHT

Chronic OHT was induced using the microbead occlusion model. A glass microneedle was inserted into a corneal puncture initially created by a 30.5-gauge needle, and 2–3 μl of 15- μm -diameter polystyrene microbeads (no. F8841; Thermo Fisher Scientific) was injected (final concentration of 2.7×10^7 beads/ml suspended in PBS). The microbeads are inert and have been used in numerous studies of experimental glaucoma (Sappington et al., 2010; Chen et al., 2011; Della Santina et al., 2013; Gao and Jakobs, 2016). This method induces an elevation in IOP that lasts 4 wk and reaches a peak of 22–27 mmHg at 4–6 d after injection. In all cases, the untreated left eye showed no increase in IOP. A separate group of mice received a saline injection in lieu of the microbeads, and they exhibited normal levels of IOP over the 30-d experimental period (Fig. S2 C; $n = 6$ per group; mean IOP over the 30 d: C57BL/6, 10.3 ± 1.1 mmHg; GFAP-STAT3-Cre⁻, 9.3 ± 1 mmHg; and GFAP-STAT3-CKO, 10.1 ± 1.2 mmHg). Mice were regularly examined on a slit lamp for signs

of any inflammatory response or overt damage in the anterior segment. Mice that showed any of these signs were excluded.

To determine whether each animal received the same degree of insult from the elevation in IOP, we calculated the area under the IOP-versus-days after injury curve (Fig. S2 D; Gao and Jakobs, 2016) using Excel (Microsoft). This area was referred to as the cIOP and gives a measure of the total pressure insult the eye was subjected to during the 30-d experimental period. Then, we measured the Δ cIOP for each animal as the cIOP of the treated eye minus the cIOP of the contralateral untreated eye (Gao and Jakobs, 2016). There was no significant difference in the Δ cIOP or peak IOP between any of the strains (Fig. S2 D).

Optic nerve crush

After anesthesia and topical corneal analgesic of mice, the optic nerve of one eye was exposed and clamped \sim 0.2 mm from the globe within the myelinated portion of the nerve (Fig. S3 E). The clamp was performed for 10 s using a self-closing jeweler's forceps (FST self-closing forceps, curved tip; Sun et al., 2010).

Measuring IOP

Mice were anaesthetized by isoflurane (2–4%; Webster Veterinary) delivered in 100% oxygen via a precision vaporizer. Measurements were taken 4–5 min after animals lost consciousness, which was defined as failure to detect motion in response to forced movement and absence of eye blinking. The IOPs were measured in both eyes 1 d before microbead injection and then every 3 d afterward using a tonometer (TONOLAB; Icare). Measurements of IOP using the tonometer match well with manometrically measured IOPs, validating this technique as precise and reproducible (Wang et al., 2005; Pease et al., 2011). Measurements were made at the same time in the morning. The tonometer takes five measurements and, based on this, gives a single mean. We considered this as one measurement; five measurements were made from each eye, and the mean was calculated to represent the IOP. IOPs were measured by individuals blinded to the genotype of the animal and the injury induced.

Retinal ganglion cell counts

Images of the whole mounted retina were obtained as z stacks (0.35- μ m step size) at a magnification of 40. Each retina was divided into quadrants, and two midperipheral regions were imaged per quadrant, for a total of eight images per retina. All cells that colocalized β III-tubulin, a ganglion cell-specific marker (Chen et al., 2011; Gao and Jakobs, 2016), and the nuclear dye DAPI were counted, and from the mean of the eight images, a ganglion cell density per retina was obtained. Percent ganglion cell loss was determined by comparing the ganglion cell density of the treated eye to the untreated contralateral eye. Cell counts were performed by individuals blinded to the genotype of the animal and the injury induced.

ERG

Full-field ERGs were recorded simultaneously from both eyes using a ColorDome system (Diagnosys LLC). Animals were dark adapted overnight (>14 h) and anesthetized, and their pupils were dilated with 1% tropicamide. Corneal anesthesia was achieved with a drop of proparacaine hydrochloride (0.5%; Akorn Inc.). Signals were recorded using gold wire loop electrodes (Diagnosys LLC). Active electrodes were precoated with GenTeal gel drops (Alcon) and placed on the center of each cornea. A reference electrode was inserted in the mouth, and a ground electrode was inserted into the tail. Animal and electrode placements were all performed under dim red light (<640 nm), which maintained dark adaptation. A heating pad was used to maintain body temperature at 37°C.

Scotopic responses were obtained for flash intensities ranging from $-3.16 \log \text{cd.s.m}^{-2}$ to $2.13 \log \text{cd.s.m}^{-2}$ in 1-log unit increments, by averaging 2–20 responses per intensity (20 for the dimmest and 2 for the brightest), with a progressively lengthened interstimulus interval of 5–60 s. This allowed for complete recovery of the b-wave amplitude. STRs were obtained for flash intensities from $-5.5 \log \text{cd.s.m}^{-2}$ to $-3 \log \text{cd.s.m}^{-2}$ by averaging 50–60 responses per intensity, with an interstimulus interval of 2 s.

For scotopic response analysis, the a-wave amplitude was measured from the baseline to the trough of the first negative wave, and the b-wave amplitude was measured from the trough of the a-wave to the peak of the first positive wave (peak-to-peak amplitude). For STR analysis, pSTR amplitude was measured from baseline to the first positive peak. ERGs were recorded before and after injury, and responses after injury were normalized to preinjury values for the same eye. ERGs were recorded by individuals blinded to the genotype of the animal and the injury induced.

Optomotor response

Visual acuity of mice was measured using an optomotor reflex-based spatial frequency threshold test (Douglas et al., 2005; Prusky et al., 2006; Della Santina et al., 2013; Gao and Jakobs, 2016). Freely moving mice were placed on a pedestal located in the center of an arena formed by four computer monitors arranged in a quadrangle. The monitors displayed a moving vertical black and white sinusoidal grating pattern. An observer, unable to see the direction of the bars, determined the direction of bar rotation by monitoring the tracking behavior of the mouse. Tracking was considered positive when there was a reproducible smooth pursuit of the head or rotation of the body in the direction concordant with the stimulus. Each eye could be tested separately depending on the direction of rotation of the grating. The staircase method was used to determine the spatial frequency at which the animal no longer responded. Rotation speed (12°/s) and contrast (100%) were kept constant. Responses were measured before and after injury by individuals blinded to the genotype of the animal and the injury induced.

Statistical analysis

For Fig. 4 (B and L) and Fig. 5, one-way ANOVA with Tukey's posttest was performed. For Figs. 7, 8, and 9, comparisons among the three mouse strains over time were done using two-way repeated-measures ANOVA with Bonferroni correction for three selected comparisons (GFAP-STAT3-CKO vs. GFAP-STAT3-Cre⁻, GFAP-STAT3-CKO vs. C57BL/6, and GFAP-STAT3-Cre⁻ vs. C57BL/6). For these figures, we have focused on whether there is a significant difference between the GFAP-STAT3-CKO and its control strain (GFAP-STAT3-Cre⁻). A p-value <0.05 was considered significant. Note that we are not comparing results across injury models but between mouse strains within each injury model. Statistical analysis was performed on the absolute numbers using Prism (v5.0; GraphPad Software).

Online supplemental material

Table S1 shows the absolute numbers for the amount of GFAP immunonegative space and process hypertrophy after astrocyte remodeling within the glial lamina. Table S2 shows the absolute numbers for the counts of ganglion cell soma and axons. Fig. S1 shows that the IOPs, ganglion cell numbers, spatial frequency threshold, and ERG of GFAP-STAT3-CKO mice are similar to their control strain and C57BL/6 mice. Fig. S2 shows that, when injected with microbeads, GFAP-STAT3-CKO and GFAP-STAT3-Cre⁻ mice undergo IOP elevation in a similar pattern to C57BL/6 mice. Fig. S3 shows that, within the optic nerve head, Cre expression was localized to astrocytes. It also shows where along the optic nerve the crush was performed.

ACKNOWLEDGMENTS

We thank Richard Masland for critical comments on this manuscript. We would also like to thank Oscar Morales for his support with the ERG and optomotor response experiments and Philip Seifert from the Histology Core Facility for assistance with the electron microscope.

This work was supported by the National Institutes of Health (grants R01 EY022092 and R01 EY019703 and core grant P30 EY003790), Research to Prevent Blindness, and the donors of National Glaucoma Research, a program of the BrightFocus Foundation.

The authors declare no competing financial interests.

Author contributions: D. Sun designed and performed the experiments. S. Moore also performed experiments. T.C. Jakobs designed the experiments and provided critical advice.

Submitted: 21 March 2016

Revised: 5 December 2016

Accepted: 8 March 2017

REFERENCES

Aaronson, D.S., and C.M. Horvath. 2002. A road map for those who don't know JAK-STAT. *Science*. 296:1653–1655. <http://dx.doi.org/10.1126/science.1071545>

Acarin, L., B. González, and B. Castellano. 2000. STAT3 and NFκB activation precedes glial reactivity in the excitotoxically injured young cortex but

not in the corresponding distal thalamic nuclei. *J. Neuropathol. Exp. Neurol.* 59:151–163. <http://dx.doi.org/10.1093/jnen/59.2.151>

- Ahmed, S.M., B.A. Rzigalinski, K.A. Willoughby, H.A. Sitterding, and E.F. Ellis. 2000. Stretch-induced injury alters mitochondrial membrane potential and cellular ATP in cultured astrocytes and neurons. *J. Neurochem.* 74:1951–1960. <http://dx.doi.org/10.1046/j.1471-4159.2000.0741951.x>
- Anderson, M.A., J.E. Burda, Y. Ren, Y. Ao, T.M. O'Shea, R. Kawaguchi, G. Coppola, B.S. Khakh, T.J. Deming, and M.V. Sofroniew. 2016. Astrocyte scar formation aids central nervous system axon regeneration. *Nature*. 532:195–200. <http://dx.doi.org/10.1038/nature17623>
- Balaratnasingam, C., W.H. Morgan, L. Bass, G. Matich, S.J. Cringle, and D.Y. Yu. 2007. Axonal transport and cytoskeletal changes in the laminar regions after elevated intraocular pressure. *Invest. Ophthalmol. Vis. Sci.* 48:3632–3644. <http://dx.doi.org/10.1167/iovs.06-1002>
- Balasingam, V., T. Tejada-Berges, E. Wright, R. Bouckova, and V.W. Yong. 1994. Reactive astrogliosis in the neonatal mouse brain and its modulation by cytokines. *J. Neurosci.* 14:846–856.
- Ben Haim, L., K. Ceyzériat, M.A. Carrillo-de Sauvage, F. Aubry, G. Auregan, M. Guillermier, M. Ruiz, F. Petit, D. Houitte, E. Faivre, et al. 2015. The JAK/STAT3 pathway is a common inducer of astrocyte reactivity in Alzheimer's and Huntington's diseases. *J. Neurosci.* 35:2817–2829. <http://dx.doi.org/10.1523/JNEUROSCI.3516-14.2015>
- Bowman, C.L., J.P. Ding, F. Sachs, and M. Sokabe. 1992. Mechanotransducing ion channels in astrocytes. *Brain Res.* 584:272–286. [http://dx.doi.org/10.1016/0006-8993\(92\)90906-P](http://dx.doi.org/10.1016/0006-8993(92)90906-P)
- Brambilla, R., V. Bracchi-Ricard, W.H. Hu, B. Frydel, A. Bramwell, S. Karmally, E.J. Green, and J.R. Bethea. 2005. Inhibition of astroglial nuclear factor κB reduces inflammation and improves functional recovery after spinal cord injury. *J. Exp. Med.* 202:145–156. <http://dx.doi.org/10.1084/jem.20041918>
- Buckingham, B.P., D.M. Inman, W. Lambert, E. Oglesby, D.J. Calkins, M.R. Steele, M.L. Vetter, N. Marsh-Armstrong, and P.J. Horner. 2008. Progressive ganglion cell degeneration precedes neuronal loss in a mouse model of glaucoma. *J. Neurosci.* 28:2735–2744. <http://dx.doi.org/10.1523/JNEUROSCI.4443-07.2008>
- Bui, B.V., B. Edmunds, G.A. Cioffi, and B. Fortune. 2005. The gradient of retinal functional changes during acute intraocular pressure elevation. *Invest. Ophthalmol. Vis. Sci.* 46:202–213. <http://dx.doi.org/10.1167/iovs.04-0421>
- Bui, B.V., A.H. Batcha, E. Fletcher, V.H. Wong, and B. Fortune. 2013. Relationship between the magnitude of intraocular pressure during an episode of acute elevation and retinal damage four weeks later in rats. *PLoS One*. 8:e70513. <http://dx.doi.org/10.1371/journal.pone.0070513>
- Burgoyne, C.F. 2011. A biomechanical paradigm for axonal insult within the optic nerve head in aging and glaucoma. *Exp. Eye Res.* 93:120–132. <http://dx.doi.org/10.1016/j.exer.2010.09.005>
- Burgoyne, C.F., J.C. Downs, A.J. Bellezza, and R.T. Hart. 2004. Three-dimensional reconstruction of normal and early glaucoma monkey optic nerve head connective tissues. *Invest. Ophthalmol. Vis. Sci.* 45:4388–4399. <http://dx.doi.org/10.1167/iovs.04-0022>
- Bush, T.G., N. Puvanachandra, C.H. Horner, A. Polito, T. Ostendorf, C.N. Svendsen, L. Mucke, M.H. Johnson, and M.V. Sofroniew. 1999. Leukocyte infiltration, neuronal degeneration, and neurite outgrowth after ablation of scar-forming, reactive astrocytes in adult transgenic mice. *Neuron*. 23:297–308. [http://dx.doi.org/10.1016/S0896-6273\(00\)80781-3](http://dx.doi.org/10.1016/S0896-6273(00)80781-3)
- Cattaneo, E., L. Conti, and C. De-Fraja. 1999. Signalling through the JAK-STAT pathway in the developing brain. *Trends Neurosci.* 22:365–369. [http://dx.doi.org/10.1016/S0166-2236\(98\)01378-2](http://dx.doi.org/10.1016/S0166-2236(98)01378-2)
- Chen, H., X. Wei, K.S. Cho, G. Chen, R. Sappington, D.J. Calkins, and D.F. Chen. 2011. Optic neuropathy due to microbead-induced elevated intraocular pressure in the mouse. *Invest. Ophthalmol. Vis. Sci.* 52:36–44. <http://dx.doi.org/10.1167/iovs.09-5115>

- Chiba, T., M. Yamada, Y. Hashimoto, M. Sato, J. Sasabe, Y. Kita, K. Terashita, S. Aiso, I. Nishimoto, and M. Matsuoka. 2005. Development of a femtomolar-acting humanin derivative named colivelin by attaching activity-dependent neurotrophic factor to its N terminus: Characterization of colivelin-mediated neuroprotection against Alzheimer's disease-relevant insults in vitro and in vivo. *J. Neurosci.* 25:10252–10261. <http://dx.doi.org/10.1523/JNEUROSCI.3348-05.2005>
- Chidlow, G., A. Ebner, J.P. Wood, and R.J. Casson. 2011. The optic nerve head is the site of axonal transport disruption, axonal cytoskeleton damage and putative axonal regeneration failure in a rat model of glaucoma. *Acta Neuropathol.* 121:737–751. <http://dx.doi.org/10.1007/s00401-011-0807-1>
- Choi, H.J., D. Sun, and T.C. Jakobs. 2015. Astrocytes in the optic nerve head express putative mechanosensitive channels. *Mol. Vis.* 21:749–766.
- Choudhury, S., Y. Liu, A.F. Clark, and I.H. Pang. 2015. Caspase-7: a critical mediator of optic nerve injury-induced retinal ganglion cell death. *Mol. Neurodegener.* 10:40. <http://dx.doi.org/10.1186/s13024-015-0039-2>
- Crowston, J.G., Y.X. Kong, I.A. Trounce, T.M. Dang, E.T. Fahy, B.V. Bui, J.C. Morrison, and V. Chrysostomou. 2015. An acute intraocular pressure challenge to assess retinal ganglion cell injury and recovery in the mouse. *Exp. Eye Res.* 141:3–8. <http://dx.doi.org/10.1016/j.exer.2015.03.006>
- Davalos, D., J. Grutzendler, G. Yang, J.V. Kim, Y. Zuo, S. Jung, D.R. Littman, M.L. Dustin, and W.B. Gan. 2005. ATP mediates rapid microglial response to local brain injury in vivo. *Nat. Neurosci.* 8:752–758. <http://dx.doi.org/10.1038/nn1472>
- Della Santina, L., D.M. Inman, C.B. Lupien, P.J. Horner, and R.O. Wong. 2013. Differential progression of structural and functional alterations in distinct retinal ganglion cell types in a mouse model of glaucoma. *J. Neurosci.* 33:17444–17457. <http://dx.doi.org/10.1523/JNEUROSCI.5461-12.2013>
- Douglas, R.M., N.M. Alam, B.D. Silver, T.J. McGill, W.W. Tschetter, and G.T. Prusky. 2005. Independent visual threshold measurements in the two eyes of freely moving rats and mice using a virtual-reality optokinetic system. *Vis. Neurosci.* 22:677–684. <http://dx.doi.org/10.1017/S0952523805225166>
- Downs, J.C., C.F. Burgoyne, W.P. Seigfried, J.F. Reynaud, N.G. Strouthidis, and V. Sallee. 2011. 24-hour IOP telemetry in the nonhuman primate: implant system performance and initial characterization of IOP at multiple timescales. *Invest. Ophthalmol. Vis. Sci.* 52:7365–7375. <http://dx.doi.org/10.1167/iovs.11-7955>
- Drögemüller, K., U. Helmuth, A. Brunn, M. Sakowicz-Burkiewicz, D.H. Gutmann, W. Mueller, M. Deckert, and D. Schlüter. 2008. Astrocyte gp130 expression is critical for the control of *Toxoplasma* encephalitis. *J. Immunol.* 181:2683–2693. <http://dx.doi.org/10.4049/jimmunol.181.4.2683>
- Faulkner, J.R., J.E. Herrmann, M.J. Woo, K.E. Tansey, N.B. Doan, and M.V. Sofroniew. 2004. Reactive astrocytes protect tissue and preserve function after spinal cord injury. *J. Neurosci.* 24:2143–2155. <http://dx.doi.org/10.1523/JNEUROSCI.3547-03.2004>
- Fields, R.D., and Y. Ni. 2010. Nonsynaptic communication through ATP release from volume-activated anion channels in axons. *Sci. Signal.* 3:ra73. <http://dx.doi.org/10.1126/scisignal.2001128>
- Fields, R.D., and B. Stevens. 2000. ATP: an extracellular signaling molecule between neurons and glia. *Trends Neurosci.* 23:625–633. [http://dx.doi.org/10.1016/S0166-2236\(00\)01674-X](http://dx.doi.org/10.1016/S0166-2236(00)01674-X)
- Fortune, B., B.V. Bui, J.C. Morrison, E.C. Johnson, J. Dong, W.O. Cepurna, L. Jia, S. Barber, and G.A. Cioffi. 2004. Selective ganglion cell functional loss in rats with experimental glaucoma. *Invest. Ophthalmol. Vis. Sci.* 45:1854–1862. <http://dx.doi.org/10.1167/iovs.03-1411>
- Frankfort, B.J., A.K. Khan, D.Y. Tse, I. Chung, J.J. Pang, Z. Yang, R.L. Gross, and S.M. Wu. 2013. Elevated intraocular pressure causes inner retinal dysfunction before cell loss in a mouse model of experimental glaucoma. *Invest. Ophthalmol. Vis. Sci.* 54:762–770. <http://dx.doi.org/10.1167/iovs.12-10581>
- Gao, S.P., and J.F. Bromberg. 2006. Touched and moved by STAT3. *Sci. STKE.* 2006:pe30. <http://dx.doi.org/10.1126/stke.3432006pe30>
- Gao, S., and T.C. Jakobs. 2016. Mice homozygous for a deletion in the glaucoma susceptibility locus INK4 show increased vulnerability of retinal ganglion cells to elevated intraocular pressure. *Am. J. Pathol.* 186:985–1005. <http://dx.doi.org/10.1016/j.ajpath.2015.11.026>
- Hamilton, N., S. Vayro, F. Kirchoff, A. Verkhatsky, J. Robbins, D.C. Gorecki, and A.M. Butt. 2008. Mechanisms of ATP- and glutamate-mediated calcium signaling in white matter astrocytes. *Glia.* 56:734–749. <http://dx.doi.org/10.1002/glia.20649>
- Haroon, F., K. Drögemüller, U. Händel, A. Brunn, D. Reinhold, G. Nishanth, W. Mueller, C. Trautwein, M. Ernst, M. Deckert, and D. Schlüter. 2011. Gp130-dependent astrocytic survival is critical for the control of autoimmune central nervous system inflammation. *J. Immunol.* 186:6521–6531. <http://dx.doi.org/10.4049/jimmunol.1001135>
- He, Z., B.V. Bui, and A.J. Vingrys. 2006. The rate of functional recovery from acute IOP elevation. *Invest. Ophthalmol. Vis. Sci.* 47:4872–4880. <http://dx.doi.org/10.1167/iovs.06-0590>
- Hernandez, M.R. 2000. The optic nerve head in glaucoma: role of astrocytes in tissue remodeling. *Prog. Retin. Eye Res.* 19:297–321. [http://dx.doi.org/10.1016/S1350-9462\(99\)00017-8](http://dx.doi.org/10.1016/S1350-9462(99)00017-8)
- Hernandez, M.R., and H. Ye. 1993. Glaucoma: changes in extracellular matrix in the optic nerve head. *Ann. Med.* 25:309–315. <http://dx.doi.org/10.3109/07853899309147290>
- Hernandez, M.R., H. Miao, and T. Lukas. 2008. Astrocytes in glaucomatous optic neuropathy. *Prog. Brain Res.* 173:353–373. [http://dx.doi.org/10.1016/S0079-6123\(08\)01125-4](http://dx.doi.org/10.1016/S0079-6123(08)01125-4)
- Herrmann, J.E., T. Imura, B. Song, J. Qi, Y. Ao, T.K. Nguyen, R.A. Korsak, K. Takeda, S. Akira, and M.V. Sofroniew. 2008. STAT3 is a critical regulator of astrogliosis and scar formation after spinal cord injury. *J. Neurosci.* 28:7231–7243. <http://dx.doi.org/10.1523/JNEUROSCI.1709-08.2008>
- Hoffman, S.W., B.A. Rzigalinski, K.A. Willoughby, and E.F. Ellis. 2000. Astrocytes generate isoprostanes in response to trauma or oxygen radicals. *J. Neurotrauma.* 17:415–420. <http://dx.doi.org/10.1089/neu.2000.17.415>
- Holcombe, D.J., N. Lengefeld, G.A. Gole, and N.L. Barnett. 2008. Selective inner retinal dysfunction precedes ganglion cell loss in a mouse glaucoma model. *Br. J. Ophthalmol.* 92:683–688. <http://dx.doi.org/10.1136/bjo.2007.133223>
- Howell, G.R., R.T. Libby, T.C. Jakobs, R.S. Smith, F.C. Phalan, J.W. Barter, J.M. Barbay, J.K. Marchant, N. Mahesh, V. Porciatti, et al. 2007. Axons of retinal ganglion cells are insulted in the optic nerve early in DBA/2J glaucoma. *J. Cell Biol.* 179:1523–1537. <http://dx.doi.org/10.1083/jcb.200706181>
- Hristova, M., E. Rocha-Ferreira, X. Fontana, L. Thei, R. Buckle, M. Christou, S. Hompoonsup, N. Gostelow, G. Raivich, and D. Peebles. 2016. Inhibition of signal transducer and activator of transcription 3 (STAT3) reduces neonatal hypoxic-ischaemic brain damage. *J. Neurochem.* 136:981–994. <http://dx.doi.org/10.1111/jnc.13490>
- Islas, L., H. Pasantes-Morales, and J.A. Sanchez. 1993. Characterization of stretch-activated ion channels in cultured astrocytes. *Glia.* 8:87–96. <http://dx.doi.org/10.1002/glia.440080204>
- Jakobs, T.C., R.T. Libby, Y. Ben, S.W. John, and R.H. Masland. 2005. Retinal ganglion cell degeneration is topological but not cell type specific in DBA/2J mice. *J. Cell Biol.* 171:313–325. <http://dx.doi.org/10.1083/jcb.200506099>
- Javid, S., A. Rezaei, and G. Karami. 2014. A micromechanical procedure for viscoelastic characterization of the axons and ECM of the brainstem.

- J. Mech. Behav. Biomed. Mater.* 30:290–299. <http://dx.doi.org/10.1016/j.jmbbm.2013.11.010>
- Jeon, C.J., E. Strettoi, and R.H. Masland. 1998. The major cell populations of the mouse retina. *J. Neurosci.* 18:8936–8946.
- John, S.W., J.R. Hagaman, T.E. MacTaggart, L. Peng, and O. Smithes. 1997. Intraocular pressure in inbred mouse strains. *Invest. Ophthalmol. Vis. Sci.* 38:249–253.
- John, S.W., R.S. Smith, O.V. Savinova, N.L. Hawes, B. Chang, D. Turnbull, M. Davisson, T.H. Roderick, and J.R. Heckenlively. 1998. Essential iris atrophy, pigment dispersion, and glaucoma in DBA/2J mice. *Invest. Ophthalmol. Vis. Sci.* 39:951–962.
- Johnson, E.C., J.C. Morrison, S. Farrell, L. Deppmeier, C.G. Moore, and M.R. McGinty. 1996. The effect of chronically elevated intraocular pressure on the rat optic nerve head extracellular matrix. *Exp. Eye Res.* 62:663–674. <http://dx.doi.org/10.1006/exer.1996.0077>
- Johnson, E.C., L. Jia, W.O. Cepurna, T.A. Doser, and J.C. Morrison. 2007. Global changes in optic nerve head gene expression after exposure to elevated intraocular pressure in a rat glaucoma model. *Invest. Ophthalmol. Vis. Sci.* 48:3161–3177. <http://dx.doi.org/10.1167/iovs.06-1282>
- Justicia, C., C. Gabriel, and A.M. Planas. 2000. Activation of the JAK/STAT pathway following transient focal cerebral ischemia: signaling through Jak1 and Stat3 in astrocytes. *Glia.* 30:253–270. [http://dx.doi.org/10.1002/\(SICI\)1098-1136\(200005\)30:3<253::AID-GLIA5>3.0.CO;2-O](http://dx.doi.org/10.1002/(SICI)1098-1136(200005)30:3<253::AID-GLIA5>3.0.CO;2-O)
- Kim, J.V., and M.L. Dustin. 2006. Innate response to focal necrotic injury inside the blood-brain barrier. *J. Immunol.* 177:5269–5277. <http://dx.doi.org/10.4049/jimmunol.177.8.5269>
- Klein, M.A., J.C. Möller, L.L. Jones, H. Bluethmann, G.W. Kreutzberg, and G. Raivich. 1997. Impaired neuroglial activation in interleukin-6 deficient mice. *Glia.* 19:227–233. [http://dx.doi.org/10.1002/\(SICI\)1098-1136\(199703\)19:3<227::AID-GLIA5>3.0.CO;2-W](http://dx.doi.org/10.1002/(SICI)1098-1136(199703)19:3<227::AID-GLIA5>3.0.CO;2-W)
- Kong, Y.X., J.G. Crowston, A.J. Vingrys, I.A. Trounce, and V.B. Bui. 2009. Functional changes in the retina during and after acute intraocular pressure elevation in mice. *Invest. Ophthalmol. Vis. Sci.* 50:5732–5740. <http://dx.doi.org/10.1167/iovs.09-3814>
- Levine, J., E. Kwon, P. Paez, W. Yan, G. Czerwiec, J.A. Loo, M.V. Sofroniew, and I.B. Wanner. 2016. Traumatically injured astrocytes release a proteomic signature modulated by STAT3-dependent cell survival. *Glia.* 64:668–694. <http://dx.doi.org/10.1002/glia.22953>
- Levison, S.W., F.J. Jiang, O.K. Stoltzfus, and M.H. Ducceschi. 2000. IL-6-type cytokines enhance epidermal growth factor-stimulated astrocyte proliferation. *Glia.* 32:328–337. [http://dx.doi.org/10.1002/1098-1136\(200012\)32:3<328::AID-GLIA110>3.0.CO;2-7](http://dx.doi.org/10.1002/1098-1136(200012)32:3<328::AID-GLIA110>3.0.CO;2-7)
- Li, R., and J.H. Liu. 2008. Telemetric monitoring of 24 h intraocular pressure in conscious and freely moving C57BL/6J and CBA/CaJ mice. *Mol. Vis.* 14:745–749.
- Li, L., A. Lundkvist, D. Andersson, U. Wilhelmsson, N. Nagai, A.C. Pardo, C. Nodin, A. Ståhlberg, K. Aprico, K. Larsson, et al. 2008. Protective role of reactive astrocytes in brain ischemia. *J. Cereb. Blood Flow Metab.* 28:468–481. <http://dx.doi.org/10.1038/sj.jcbfm.9600546>
- Li, Y., C.L. Schlamp, and R.W. Nickells. 1999. Experimental induction of retinal ganglion cell death in adult mice. *Invest. Ophthalmol. Vis. Sci.* 40:1004–1008.
- Libby, R.T., M.G. Anderson, I.H. Pang, Z.H. Robinson, O.V. Savinova, I.M. Cosma, A. Snow, L.A. Wilson, R.S. Smith, A.F. Clark, and S.W. John. 2005. Inherited glaucoma in DBA/2J mice: pertinent disease features for studying the neurodegeneration. *Vis. Neurosci.* 22:637–648. <http://dx.doi.org/10.1017/S0952523805225130>
- Liu, X., Y. Tian, N. Lu, T. Gin, C.H. Cheng, and M.T. Chan. 2013. Stat3 inhibition attenuates mechanical allodynia through transcriptional regulation of chemokine expression in spinal astrocytes. *PLoS One.* 8:e75804. <http://dx.doi.org/10.1371/journal.pone.0075804>
- Liu, Y., C.M. McDowell, Z. Zhang, H.E. Tebow, R.J. Wordinger, and A.F. Clark. 2014. Monitoring retinal morphologic and functional changes in mice following optic nerve crush. *Invest. Ophthalmol. Vis. Sci.* 55:3766–3774. <http://dx.doi.org/10.1167/iovs.14-13895>
- Lye-Barthel, M., D. Sun, and T.C. Jakobs. 2013. Morphology of astrocytes in a glaucomatous optic nerve. *Invest. Ophthalmol. Vis. Sci.* 54:909–917. <http://dx.doi.org/10.1167/iovs.12-10109>
- Matsuoka, M., Y. Hashimoto, S. Aiso, and I. Nishimoto. 2006. Humanin and colivelin: neuronal-death-suppressing peptides for Alzheimer's disease and amyotrophic lateral sclerosis. *CNS Drug Rev.* 12:113–122. <http://dx.doi.org/10.1111/j.1527-3458.2006.00113.x>
- May, C.A., and E. Lütjen-Drecoll. 2002. Morphology of the murine optic nerve. *Invest. Ophthalmol. Vis. Sci.* 43:2206–2212.
- McKinnon, S.J., C.L. Schlamp, and R.W. Nickells. 2009. Mouse models of retinal ganglion cell death and glaucoma. *Exp. Eye Res.* 88:816–824. <http://dx.doi.org/10.1016/j.exer.2008.12.002>
- Minckler, D.S., A.H. Bunt, and G.W. Johanson. 1977. Orthograde and retrograde axoplasmic transport during acute ocular hypertension in the monkey. *Invest. Ophthalmol. Vis. Sci.* 16:426–441.
- Morrison, J.C., M.E. Dorman-Pease, G.R. Dunkelberger, and H.A. Quigley. 1990. Optic nerve head extracellular matrix in primary optic atrophy and experimental glaucoma. *Arch. Ophthalmol.* 108:1020–1024. <http://dx.doi.org/10.1001/archophth.1990.01070090122053>
- Myer, D.J., G.G. Gurkoff, S.M. Lee, D.A. Hovda, and M.V. Sofroniew. 2006. Essential protective roles of reactive astrocytes in traumatic brain injury. *Brain.* 129:2761–2772. <http://dx.doi.org/10.1093/brain/awl165>
- Neary, J.T., Y. Kang, K.A. Willoughby, and E.F. Ellis. 2003. Activation of extracellular signal-regulated kinase by stretch-induced injury in astrocytes involves extracellular ATP and P2 purinergic receptors. *J. Neurosci.* 23:2348–2356.
- Neary, J.T., Y. Kang, M. Tran, and J. Feld. 2005. Traumatic injury activates protein kinase B/Akt in cultured astrocytes: role of extracellular ATP and P2 purinergic receptors. *J. Neurotrauma.* 22:491–500. <http://dx.doi.org/10.1089/neu.2005.22.491>
- Nickells, R.W., G.R. Howell, I. Soto, and S.W. John. 2012. Under pressure: cellular and molecular responses during glaucoma, a common neurodegeneration with axonopathy. *Annu. Rev. Neurosci.* 35:153–179. <http://dx.doi.org/10.1146/annurev.neuro.051508.135728>
- Nobuta, H., C.A. Ghiani, P.M. Paez, V. Spreuer, H. Dong, R.A. Korsak, A. Manukyan, J. Li, H.V. Vinters, E.J. Huang, et al. 2012. STAT3-mediated astrogliosis protects myelin development in neonatal brain injury. *Ann. Neurol.* 72:750–765. <http://dx.doi.org/10.1002/ana.23670>
- O'Callaghan, J.P., K.A. Kelly, R.L. VanGilder, M.V. Sofroniew, and D.B. Miller. 2014. Early activation of STAT3 regulates reactive astrogliosis induced by diverse forms of neurotoxicity. *PLoS One.* 9:e102003. <http://dx.doi.org/10.1371/journal.pone.0102003>
- Okada, S., M. Nakamura, H. Katoh, T. Miyao, T. Shimazaki, K. Ishii, J. Yamane, A. Yoshimura, Y. Iwamoto, Y. Toyama, and H. Okano. 2006. Conditional ablation of Stat3 or Socs3 discloses a dual role for reactive astrocytes after spinal cord injury. *Nat. Med.* 12:829–834. <http://dx.doi.org/10.1038/nm1425>
- Ostrow, L.W., T.M. Suchyna, and F. Sachs. 2011. Stretch induced endothelin-1 secretion by adult rat astrocytes involves calcium influx via stretch-activated ion channels (SACs). *Biochem. Biophys. Res. Commun.* 410:81–86. <http://dx.doi.org/10.1016/j.bbrc.2011.05.109>
- Pan, H., H. Wang, X. Wang, L. Zhu, and L. Mao. 2012. The absence of Nrf2 enhances NF-κB-dependent inflammation following scratch injury in mouse primary cultured astrocytes. *Mediators Inflamm.* 2012:217580. <http://dx.doi.org/10.1155/2012/217580>
- Pascolini, D., and S.P. Mariotti. 2012. Global estimates of visual impairment: 2010. *Br. J. Ophthalmol.* 96:614–618. <http://dx.doi.org/10.1136/bjophthalmol-2011-300539>

- Pease, M.E., S.J. McKinnon, H.A. Quigley, L.A. Kerrigan-Baumrind, and D.J. Zack. 2000. Obstructed axonal transport of BDNF and its receptor TrkB in experimental glaucoma. *Invest. Ophthalmol. Vis. Sci.* 41:764–774.
- Pease, M.E., F.E. Cone, S. Gelman, J.L. Son, and H.A. Quigley. 2011. Calibration of the TonoLab tonometer in mice with spontaneous or experimental glaucoma. *Invest. Ophthalmol. Vis. Sci.* 52:858–864. <http://dx.doi.org/10.1167/iiov.10-5556>
- Pérez de Lara, M.J., C. Santano, A. Guzmán-Aránguez, F.J. Valiente-Soriano, M. Avilés-Trigueros, M. Vidal-Sanz, P. de la Villa, and J. Pintor. 2014. Assessment of inner retina dysfunction and progressive ganglion cell loss in a mouse model of glaucoma. *Exp. Eye Res.* 122:40–49. <http://dx.doi.org/10.1016/j.exer.2014.02.022>
- Pettus, E.H., and J.T. Povlishock. 1996. Characterization of a distinct set of intra-axonal ultrastructural changes associated with traumatically induced alteration in axolemmal permeability. *Brain Res.* 722:1–11. [http://dx.doi.org/10.1016/0006-8993\(96\)00113-8](http://dx.doi.org/10.1016/0006-8993(96)00113-8)
- Porciatti, V. 2015. Electrophysiological assessment of retinal ganglion cell function. *Exp. Eye Res.* 141:164–170. <http://dx.doi.org/10.1016/j.exer.2015.05.008>
- Prusky, G.T., N.M. Alam, and R.M. Douglas. 2006. Enhancement of vision by monocular deprivation in adult mice. *J. Neurosci.* 26:11554–11561. <http://dx.doi.org/10.1523/JNEUROSCI.3396-06.2006>
- Qu, J., and T.C. Jakobs. 2013. The time course of gene expression during reactive gliosis in the optic nerve. *PLoS One.* 8:e67094. <http://dx.doi.org/10.1371/journal.pone.0067094>
- Quigley, H.A. 1999. Neuronal death in glaucoma. *Prog. Retin. Eye Res.* 18:39–57. [http://dx.doi.org/10.1016/S1350-9462\(98\)00014-7](http://dx.doi.org/10.1016/S1350-9462(98)00014-7)
- Quigley, H.A. 2011. Glaucoma. *Lancet.* 377:1367–1377. [http://dx.doi.org/10.1016/S0140-6736\(10\)61423-7](http://dx.doi.org/10.1016/S0140-6736(10)61423-7)
- Quigley, H.A., M.E. Dorman-Pease, and A.E. Brown. 1991. Quantitative study of collagen and elastin of the optic nerve head and sclera in human and experimental monkey glaucoma. *Curr. Eye Res.* 10:877–888. <http://dx.doi.org/10.3109/02713689109013884>
- Rabchevsky, A.G., J.M. Weinitz, M. Culpier, C. Fages, M. Tinel, and M.P. Junier. 1998. A role for transforming growth factor α as an inducer of astrogliosis. *J. Neurosci.* 18:10541–10552.
- Ralay Ranaivo, H., S.M. Zunich, N. Choi, J.N. Hodge, and M.S. Wainwright. 2011. Mild stretch-induced injury increases susceptibility to interleukin-1 β -induced release of matrix metalloproteinase-9 from astrocytes. *J. Neurotrauma.* 28:1757–1766. <http://dx.doi.org/10.1089/neu.2011.1799>
- Roth, T.L., D. Nayak, T. Atanasijevic, A.P. Koretsky, L.L. Latour, and D.B. McGavern. 2014. Transcranial amelioration of inflammation and cell death after brain injury. *Nature.* 505:223–228. <http://dx.doi.org/10.1038/nature12808>
- Ryu, M., M. Yasuda, D. Shi, A.Y. Shanab, R. Watanabe, N. Himori, K. Omodaka, Y. Yokoyama, J. Takano, T. Saïdo, and T. Nakazawa. 2012. Critical role of calpain in axonal damage-induced retinal ganglion cell death. *J. Neurosci. Res.* 90:802–815. <http://dx.doi.org/10.1002/jnr.22800>
- Rzagalinski, B.A., S. Liang, J.S. McKinney, K.A. Willoughby, and E.F. Ellis. 1997. Effect of Ca²⁺ on in vitro astrocyte injury. *J. Neurochem.* 68:289–296. <http://dx.doi.org/10.1046/j.1471-4159.1997.68010289.x>
- Saleh, M., M. Nagaraju, and V. Porciatti. 2007. Longitudinal evaluation of retinal ganglion cell function and IOP in the DBA/2J mouse model of glaucoma. *Invest. Ophthalmol. Vis. Sci.* 48:4564–4572. <http://dx.doi.org/10.1167/iiov.07-0483>
- Sappington, R.M., B.J. Carlson, S.D. Crish, and D.J. Calkins. 2010. The microbead occlusion model: a paradigm for induced ocular hypertension in rats and mice. *Invest. Ophthalmol. Vis. Sci.* 51:207–216. <http://dx.doi.org/10.1167/iiov.09-3947>
- Schlamp, C.L., Y. Li, J.A. Dietz, K.T. Janssen, and R.W. Nickells. 2006. Progressive ganglion cell loss and optic nerve degeneration in DBA/2J mice is variable and asymmetric. *BMC Neurosci.* 7:66. <http://dx.doi.org/10.1186/1471-2202-7-66>
- Shiratori-Hayashi, M., K. Koga, H. Tozaki-Saitoh, Y. Kohro, H. Toyonaga, C. Yamaguchi, A. Hasegawa, T. Nakahara, J. Hachisuka, S. Akira, et al. 2015. STAT3-dependent reactive astrogliosis in the spinal dorsal horn underlies chronic itch. *Nat. Med.* 21:927–931. <http://dx.doi.org/10.1038/nm.3912>
- Singleton, R.H., and J.T. Povlishock. 2004. Identification and characterization of heterogeneous neuronal injury and death in regions of diffuse brain injury: evidence for multiple independent injury phenotypes. *J. Neurosci.* 24:3543–3553. <http://dx.doi.org/10.1523/JNEUROSCI.5048-03.2004>
- Sofroniew, M.V. 2009. Molecular dissection of reactive astrogliosis and glial scar formation. *Trends Neurosci.* 32:638–647. <http://dx.doi.org/10.1016/j.tins.2009.08.002>
- Sofroniew, M.V., and H.V. Vinters. 2010. Astrocytes: biology and pathology. *Acta Neuropathol.* 119:7–35. <http://dx.doi.org/10.1007/s00401-009-0619-8>
- Soto, I., E. Oglesby, B.P. Buckingham, J.L. Son, E.D. Roberson, M.R. Steele, D.M. Inman, M.L. Vetter, P.J. Horner, and N. Marsh-Armstrong. 2008. Retinal ganglion cells downregulate gene expression and lose their axons within the optic nerve head in a mouse glaucoma model. *J. Neurosci.* 28:548–561. <http://dx.doi.org/10.1523/JNEUROSCI.3714-07.2008>
- Sriram, K., S.A. Benkovic, M.A. Hebert, D.B. Miller, and J.P. O’Callaghan. 2004. Induction of gp130-related cytokines and activation of JAK2/STAT3 pathway in astrocytes precedes up-regulation of glial fibrillary acidic protein in the 1-methyl-4-phenyl-1,2,3,6-tetrahydropyridine model of neurodegeneration: key signaling pathway for astrogliosis in vivo? *J. Biol. Chem.* 279:19936–19947. <http://dx.doi.org/10.1074/jbc.M309304200>
- Sun, D., and T.C. Jakobs. 2012. Structural remodeling of astrocytes in the injured CNS. *Neuroscientist.* 18:567–588. <http://dx.doi.org/10.1177/1073858411423441>
- Sun, D., M. Lye-Barthel, R.H. Masland, and T.C. Jakobs. 2009. The morphology and spatial arrangement of astrocytes in the optic nerve head of the mouse. *J. Comp. Neurol.* 516:1–19. <http://dx.doi.org/10.1002/cne.22058>
- Sun, D., M. Lye-Barthel, R.H. Masland, and T.C. Jakobs. 2010. Structural remodeling of fibrous astrocytes after axonal injury. *J. Neurosci.* 30:14008–14019. <http://dx.doi.org/10.1523/JNEUROSCI.3605-10.2010>
- Sun, D., J. Qu, and T.C. Jakobs. 2013. Reversible reactivity by optic nerve astrocytes. *Glia.* 61:1218–1235. <http://dx.doi.org/10.1002/glia.22507>
- Takeda, K., T. Kaisho, N. Yoshida, J. Takeda, T. Kishimoto, and S. Akira. 1998. Stat3 activation is responsible for IL-6-dependent T cell proliferation through preventing apoptosis: generation and characterization of T cell-specific Stat3-deficient mice. *J. Immunol.* 161:4652–4660.
- Tsuda, M., Y. Kohro, T. Yano, T. Tsujikawa, J. Kitano, H. Tozaki-Saitoh, S. Koyanagi, S. Ohdo, R.R. Ji, M.W. Salter, and K. Inoue. 2011. JAK-STAT3 pathway regulates spinal astrocyte proliferation and neuropathic pain maintenance in rats. *Brain.* 134:1127–1139. <http://dx.doi.org/10.1093/brain/awr025>
- Verderio, C., and M. Matteoli. 2001. ATP mediates calcium signaling between astrocytes and microglial cells: modulation by IFN- γ . *J. Immunol.* 166:6383–6391. <http://dx.doi.org/10.4049/jimmunol.166.10.6383>
- Voskuhl, R.R., R.S. Peterson, B. Song, Y. Ao, L.B. Morales, S. Tiwari-Woodruff, and M.V. Sofroniew. 2009. Reactive astrocytes form scar-like perivascular barriers to leukocytes during adaptive immune inflammation of the CNS. *J. Neurosci.* 29:11511–11522. <http://dx.doi.org/10.1523/JNEUROSCI.1514-09.2009>
- Wang, J., G. Li, Z. Wang, X. Zhang, L. Yao, F. Wang, S. Liu, J. Yin, E.A. Ling, L. Wang, and A. Hao. 2012b. High glucose-induced expression of inflammatory cytokines and reactive oxygen species in cultured

- astrocytes. *Neuroscience*. 202:58–68. <http://dx.doi.org/10.1016/j.neuroscience.2011.11.062>
- Wang, W.H., J.C. Millar, I.H. Pang, M.B. Wax, and A.F. Clark. 2005. Noninvasive measurement of rodent intraocular pressure with a rebound tonometer. *Invest. Ophthalmol. Vis. Sci.* 46:4617–4621. <http://dx.doi.org/10.1167/iops.05-0781>
- Wang, X., P.J. Crowe, D. Goldstein, and J.L. Yang. 2012a. STAT3 inhibition, a novel approach to enhancing targeted therapy in human cancers (review). *Int. J. Oncol.* 41:1181–1191. <http://dx.doi.org/10.3892/ijo.2012.1568>
- Wanner, I.B., M.A. Anderson, B. Song, J. Levine, A. Fernandez, Z. Gray-Thompson, Y. Ao, and M.V. Sofroniew. 2013. Glial scar borders are formed by newly proliferated, elongated astrocytes that interact to corral inflammatory and fibrotic cells via STAT3-dependent mechanisms after spinal cord injury. *J. Neurosci.* 33:12870–12886. <http://dx.doi.org/10.1523/JNEUROSCI.2121-13.2013>
- Winter, C.G., Y. Saotome, S.W. Levison, and D. Hirsh. 1995. A role for ciliary neurotrophic factor as an inducer of reactive gliosis, the glial response to central nervous system injury. *Proc. Natl. Acad. Sci. USA.* 92:5865–5869. <http://dx.doi.org/10.1073/pnas.92.13.5865>
- Wong, M., Y. Li, S. Li, S. Zhang, W. Li, P. Zhang, C. Chen, C.J. Barnstable, S.S. Zhang, C. Zhang, and P. Huang. 2015. Therapeutic retrobulbar inhibition of STAT3 protects ischemic retina ganglion cells. *Mol. Neurobiol.* 52:1364–1377. <http://dx.doi.org/10.1007/s12035-014-8945-9>
- Wu, M.N., L.W. Zhou, Z.J. Wang, W.N. Han, J. Zhang, X.J. Liu, J.Q. Tong, and J.S. Qi. 2015. Colivelin ameliorates amyloid β peptide-induced impairments in spatial memory, synaptic plasticity, and calcium homeostasis in rats. *Hippocampus*. 25:363–372. <http://dx.doi.org/10.1002/hipo.22378>
- Yamauchi, K., K. Osuka, M. Takayasu, N. Usuda, A. Nakazawa, N. Nakahara, M. Yoshida, C. Aoshima, M. Hara, and J. Yoshida. 2006. Activation of JAK/STAT signalling in neurons following spinal cord injury in mice. *J. Neurochem.* 96:1060–1070. <http://dx.doi.org/10.1111/j.1471-4159.2005.03559.x>
- Yu, H., and R. Jove. 2004. The STATs of cancer—new molecular targets come of age. *Nat. Rev. Cancer*. 4:97–105. <http://dx.doi.org/10.1038/nrc1275>
- Zamanian, J.L., L. Xu, L.C. Foo, N. Nouri, L. Zhou, R.G. Giffard, and B.A. Barres. 2012. Genomic analysis of reactive astrogliosis. *J. Neurosci.* 32:6391–6410. <http://dx.doi.org/10.1523/JNEUROSCI.6221-11.2012>
- Zhang, S., W. Li, W. Wang, S.S. Zhang, P. Huang, and C. Zhang. 2013. Expression and activation of STAT3 in the astrocytes of optic nerve in a rat model of transient intraocular hypertension. *PLoS One*. 8:e55683. <http://dx.doi.org/10.1371/journal.pone.0055683>